Available online at www.sciencedirect.com
SCIENCE DIRECT®
Bioorganic Chemistry 32 (2004) 393–437
BIOORGANIC CHEMISTRY
www.elsevier.com/locate/bioorg

Mini-review

Elucidation of enzyme mechanisms using fluorinated substrate analogues

Rongson Pongdee, Hung-wen Liu*

Division of Medicinal Chemistry, Department of Chemistry and Biochemistry, College of Pharmacy, University of Texas, Austin, TX 78712, USA

Received 17 June 2004

Abstract

A great variety of biological reactions that are physiologically important are catalyzed by enzymes. Understanding the reaction course of these enzyme-catalyzed transformations are of significant importance since the insights gained from these experiments may facilitate the design of methods to control or mimic their actions. A common strategy to study enzyme catalyses is to use fluorinated substrate analogues as mechanistic probes, since fluorine is an effective hydroxyl group mimic and can also be used to replace a hydrogen atom. Using fluorinated substrate probes have enabled researchers to obtain crucial information regarding the catalytic mechanism of enzymatic reactions. Many of these compounds are good enzyme inhibitors and have been developed into clinically useful chemotherapeutic agents. This review will discuss some examples of the use of fluorine containing compounds as mechanistic probes/enzyme inhibitors, many of which are selected from our own work.

Keyword: Fluorinated substrates

* Corresponding author. Fax: +1 512 471 2746.
E-mail address: h.w.liu@mail.utexas.edu (H. Liu).

0045-2068/$ - see front matter
doi:10.1016/j.bioorg.2004.06.012

1. Introduction

The use of fluorinated substrates as mechanistic probes and inhibitors has proven to be a powerful method for obtaining information about the catalytic mechanism of various enzymatic transformations [1,2]. The unique stereoelectronic properties of the fluorine atom make it an effective bioisostere for both the hydrogen and oxygen atom. The electronegativity and van der Waals radii of fluorine (4.0, 1.47 Å) compare favorably with those of oxygen (3.5, 1.57 Å) allowing fluorine to serve as an effective hydroxyl group mimic [3]. The use of fluorine as a hydrogen surrogate is somewhat less intuitive, since the van der Waals radii of hydrogen (1.2 Å) is much smaller than that of fluorine. However, analysis of monofluorinated stearic acids deposited on graphite reveals a smooth two-dimensional packing suggesting a very close isosteric relationship between hydrogen and fluorine [4]. Thus, fluorine has also been used to replace hydrogen atoms in designing enzyme probes and inhibitors.

This review will not provide an exhaustive account of the use of fluorine containing substrates as mechanistic probes or inhibitors. Rather, it will highlight a few representative examples from the literature where the utilization of fluorinated substrates played a key role in establishing the mechanistic course of an enzymatic reaction, including some examples of our own work in this area. The review is divided into the three reaction classes: cationic, oxidation–reduction, and radical, where fluorinated analogues have been used as mechanistic probes. A miscellaneous section encompassing all other reaction types is also included.

2. Cationic mechanisms

2.1. Prenyltransferases

Terpenes, exemplified by the sterols, carotenes, dolichols, and other respiratory coenzymes, represent the largest class of natural products with nearly 35,000 members. They have their biogenetic origins in either the classical mevalonate pathway beginning from acetyl-CoA (**1**), or the more recently discovered non-mevalonate pathway originating from glyceraldehyde 3-phosphate (**2**) [5,6]. The fundamental step in terpene biosynthesis is catalyzed by a family of enzymes broadly classified as prenyltransferases. This enzyme class is responsible for the condensation of isopentenyl pyrophosphate (IPP, **3**) with another allylic pyrophosphate unit **4** to construct elongated isoprenoids **5** as shown in Scheme 1.

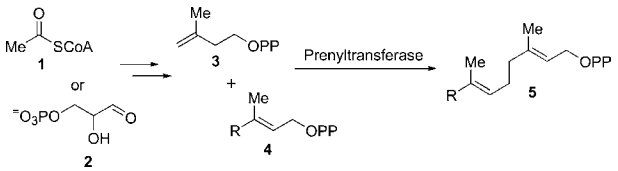

Scheme 1.

Two mechanistic routes have been proposed to account for the chain elongation catalyzed by prenyltransferases as depicted in Scheme 2. In mechanism A, a concerted S_N2-like displacement of the C(1′)-phosphate by the C(3)–C(4) olefin of IPP (**3**) facilitated by an enzyme active site residue furnishes the covalently bound intermediate **6** [7,8]. Next, *trans*-elimination involving removal of a C(2)-hydrogen would generate the extended terpene (**5**). On the other hand, ionization of the C(1′)-phosphate, possibly assisted by the neighboring olefin, would result in the allylic cation **7** as shown in mechanism B [8–10]. A Prins-like reaction involving the terminal olefin of IPP (**3**) and the allylic cation **7**, followed by abstraction of the C(2)-hydrogen, would then afford **5**.

Early stereochemical investigations by Cornforth revealed that the displacement of the C(1′)-phosphate occurred with inversion of configuration and that the allylic pyrophosphate **4** approached from the *si*-face of IPP (**3**) [8]. In addition, the stereochemistry of the newly generated olefin in the elongated isoprenoid **5** was found to be dependent upon the removal of either the C(2)-*pro*-(*R*) or *pro*-(*S*) hydrogen of IPP (**3**) [8]. In other words, prenyltransferases which generate *E* alkenes remove H_R and those that generate *Z* alkenes abstract H_S. These stereochemical requirements were considered to support the "elimination–displacement" mechanism (mechanism A) shown in Scheme 2. In this mechanism, the participation of a hypothetical X-group may be necessary to direct the stereochemical course of the reaction.

However, the discovery by Poulter that avian liver prenyltransferase catalyzes the hydrolysis of an allylic pyrophosphate in the absence of IPP (**3**) led to a reexamination of the widely accepted "displacement-elimination" mechanism [7,8]. Incubation of porcine liver prenyltransferase and geranyl pyrophosphate with $H_2{}^{18}O$ in the absence of IPP (**3**) resulted in a nearly quantitative incorporation of the ^{18}O label in the hydrolysis product, geraniol [11]. This observation established that the C–O bond of geranyl pyrophosphate had been cleaved during the enzymatic reaction. More importantly, further experiments eliminated the possibility that the reaction in the absence of IPP (**3**) was due to a phosphatase-like activity and gave strong evidence in support of an "ionization–condensation–elimination" pathway as shown in Scheme 2 (mechanism B) [9].

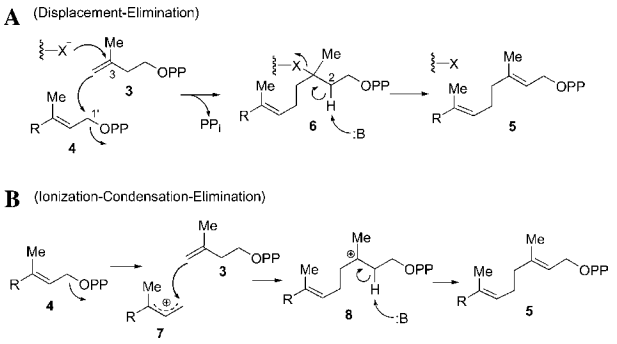

Scheme 2.

Mechanistic studies were then performed with the dimethylally pyrophosphate (DMAPP) analogues, (*E*)-(**9**) and (*Z*)-3-trifluoromethyl-2-buten-1-yl pyrophosphate (**10**, Fig. 1) [12]. These substrates were chosen for two reasons: they were not expected to perturb the conformation of the enzyme's active site since the steric size of a methyl and trifluoromethyl group are similar, and substitution of a methyl for a trifluoromethyl group ($\sigma^* = 0.612$) would dramatically destabilize a carbocation transition state and severely retard the rate of an S_N1-like process [13]. The rate predictions were verified from model systems involving the direct displacement and solvolysis of methanesulfonate ester derivatives of both DMAPP (**11**) and the trifluorinated analogues **9** and **10** [12]. Incubation of **9** and **10** with porcine liver prenyltransferase resulted in a reaction rate that was 3×10^7 times slower compared with that of the natural substrate DMAPP (**11**). While this result was initially viewed as evidence in support of the "ionization–condensation–elimination" mechanism, some problems associated with the use of **9** and **10** as substrate analogues precluded a definitive conclusion.

First, the inhibition constants for the trifluorinated analogues, K_i (**9**) = 51 μM and the K_i (**10**) = 62 μM, were substantially larger than that of DMAPP (**11**) indicating a reduced affinity of **9** and **10** for the enzyme. Second, the extremely slow reaction rate precluded the isolation and characterization of any products to verify that the fluorinated analogues were turned over by the enzyme. To circumvent these problems, Poulter synthesized the 2-fluorogeranyl pyrophosphate analogue (**12**, Fig. 1) [14,15]. When the monofluorinated pyrophosphate **12** was incubated with isopentenyl-^{14}C pyrophosphate and porcine liver farnesyl pyrophosphate synthetase, the rate of reaction was suppressed ($k_{cat} = 8.4 \times 10^{-4}$) with a K_m of 1.1 μM [15]. 2-Fluorogeranyl pyrophosphate (**12**) also behaved as a competitive inhibitor with a $K_i = 2.4$ μM. Hence, the binding affinity for **12** is comparable to that of the natural substrate ($K_m = 0.8$ μM) confirming that the slow turnover was not due to poor binding. Additionally, the product of the reaction was identified as 6-fluoro-farnesyl pyrophosphate by GC/MS analysis thereby establishing unambiguously that this, and likely all, prenyltransferases proceed via a cationic transition state.

2.2. Isopentenyl pyrophosphate Type I isomerase

The pathway comprising the biosynthesis of isoprenoid natural products contains a number of enzymes catalyzing novel transformations [5,6]. One enzyme present in both the mevalonate (Type I) and non-mevalonate (Type II) pathways is isopentenyl pyrophosphate isomerase (IPP isomerase). While no mechanistic studies have been reported for the Type II enzyme, the Type I enzyme has been the subject of intense investigation. IPP isomerase converts isopentenyl pyrophosphate (**3**) to its activated

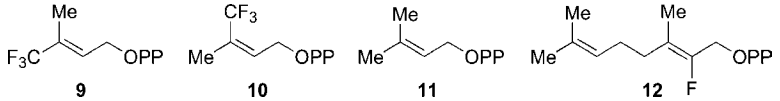

Fig. 1. Structures of DMAPP and fuorinated analogues of allylic pyrophosphates.

allylic counterpart dimethylallyl pyrophosphate (DMAPP, **11**, Scheme 3), which serves as the electrophilic component in subsequent prenyl transfer reactions.

Early mechanistic studies of the incubation of IPP isomerase in $^{3}H_2O$ revealed that the C(2)-*pro*-(*R*)-hydrogen of IPP (**3**) is lost to water and that a proton from water is added to the *si*-face of IPP (**3**) at C(4) to form DMAPP (**11**) [16]. This result is consistent with a carbocation mechanism in which protonation of the terminal olefin of IPP (**3**) leads to the transient tertiary carbocation **13**. DMAPP (**11**) is then formed by subsequent loss of a C(2)-hydrogen. However, a route involving a carbanion intermediate could not be excluded based solely on this information. For example, deprotonation of a C(2)-hydrogen would result in the allylic carbanion **14** which upon reprotonation would form DMAPP (**11**). Both of these pathways are depicted in Scheme 4.

Independent studies by Abeles, using the enzyme from Baker's yeast, and Poulter, using the enzyme from the mold *Claviceps purpurea*, further clarified the mechanism of IPP isomerase. Initial mechanistic investigations by both laboratories used 2-(dimethylamino)ethyl pyrophosphate (NIPP, **15**, Fig. 2) [17,18], which had previously been identified as a potent inhibitor of squalene synthetase, bornyl-diphosphate cyclase, and sterol methylases. The potent inhibition could result from mimicking the carbocationic transition states of these enzyme-catalyzed reactions [19–23]. Therefore, it was expected that NIPP (**15**) would also function as a potent inhibitor for IPP isomerase if the reaction proceeds via a carbocation intermediate.

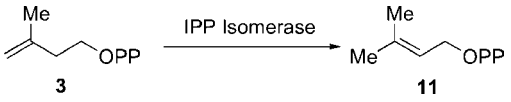

Scheme 3.

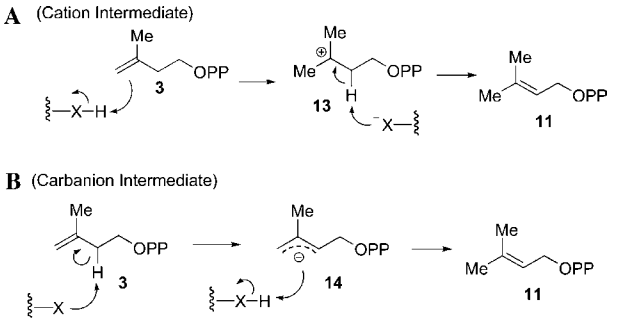

Scheme 4.

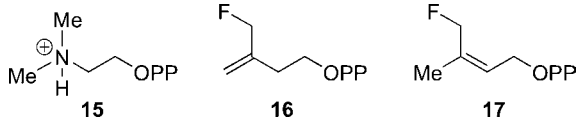

Fig. 2. Structures of substrate analogues for IPP (Type I) isomerase.

Both Abeles and Poulter observed a time-dependent inactivation upon incubation of the ammonium analogue NIPP (**15**) with IPP isomerase [17,18]. In each case, inhibition was viewed as irreversible with a $K_i \leqslant 1.4 \times 10^{-11}$ M for the enzyme from Baker's yeast and a $K_i \leqslant 1.2 \times 10^{-10}$ M for the *C. purpurea* enzyme. While binding was extremely tight, inhibition was not due to covalent attachment as enzyme activity was restored in both enzymes by treating the inactivated enzyme complex with either 6 M urea or a 2-mercaptoethanol solution containing 0.5% SDS, respectively. More likely, the inhibition was the result of tight binding of NIPP (**15**) through electrostatic interactions of the ammonium nitrogen with a negatively charged residue in the active site.

Further evidence supporting a carbocation intermediate in the IPP isomerase-catalyzed reaction came from incubation studies using (*Z*)-3-trifluoromethyl-2-butenyl pyrophosphate (**10**, Fig. 1) [24]. Abeles found that the turnover of IPP isomerase was severely reduced ($k_{cat} = 1.8 \times 10^{-6}$) when incubated with the trifluorinated analogue **10**. This value is consistent with prior results obtained by Poulter on the inhibition of prenyltransfer reactions with **10** and further implicates a cationic transition state [13].

Poulter also attempted to determine the effects of fluorinated derivatives on the k_{cat} of IPP isomerase employing monofluorinated FIPP (**16**) and FDMAPP (**17**, Fig. 2) [18,25]. However, FIPP (**16**) and FDMAPP (**17**) were not substrates for the enzyme. Rather, they resulted in covalent modification of IPP isomerase. Covalent attachment was proposed to occur by direct displacement of the fluorine residue in either an S_N2 or S_N2' fashion as determined by spectrophotometric detection of fluoride ion in a 1:1 ratio with enzyme present in the reaction mixture. The actual mechanism of fluoride release was later confirmed to be via an S_N2 pathway [26]. Further site-directed mutagenesis experiments established that the two catalytic residues involved in IPP isomerase were Cys139 and Glu207 [27].

2.3. Glycosidases

Glycosidases, enzymes responsible for the cleavage of glycosidic linkages in carbohydrates, are involved in numerous biological processes and have garnered attention as potential therapeutic targets for the treatment of diabetes and many other diseases. The hydrolysis reaction catalyzed by "retaining" glycosidases, those which preserve the stereochemistry at the anomeric position, involves formation of a covalent adduct between the sugar and an enzyme active site residue (Scheme 5). Subsequent glycosylation of the enzyme bound sugar releases the product glycoside and regenerates the active site residue. Both steps in this mechanism are widely accepted to proceed via transition states with significant oxonium ion (**20**)-like character.

In an effort to identify the active site residues involved in catalysis by "retaining" glycosidases, Withers designed the fluorinated glycosides shown in Fig. 3 as mechanism-based inhibitors [28–30]. Since the putative intermediates of these enzymatic reactions possess substantial cationic character, it was anticipated that the substitution of a fluorine atom for a hydroxy group at the C(2)-position would severely retard the rate of both the glycolysis and the glycosylation steps. However, the

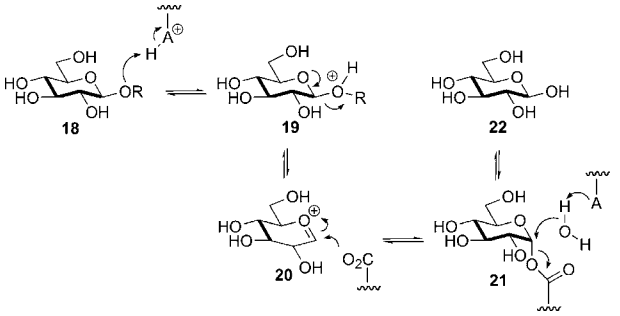

Scheme 5.

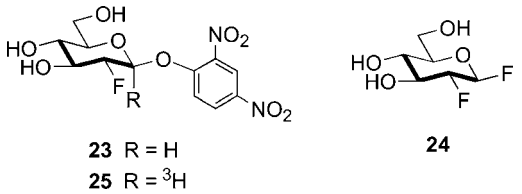

Fig. 3. Structures of mechanism-based glycosidase inhibitors.

incorporation of a highly reactive leaving group (fluoride or dinitrophenolate) could offset the expected rate reduction on the glycolysis step (**19** → **20**) allowing for sufficient accumulation of the enzyme bound intermediate **21**, which would result in temporary inactivation of the enzyme.

The initial studies aimed at ascertaining the ability of 2-deoxy-2-fluoroglycosides to serve as mechanism-based inhibitors involved incubation studies of **23** with *A. faecalis* β-glucosidase [28]. Those experiments revealed a rapid time-dependent inactivation of the enzyme with a dissociation constant (K_i) of 0.05 mM and a rate constant (k_i) of 25 min^{-1}. The inhibitory effects of **23** could be reversed by adding the competitive inhibitor isopropyl β-D-glucopyranoside indicating that **23** is likely interacting at the enzyme active site.

Further incubation experiments involving **24** led to the characterization of a covalent enzyme-inhibitor adduct validating the presence of such an intermediate during normal catalysis [29]. Monitoring of the reaction by ^{19}F NMR spectroscopy showed three resonances at δ 121.0, 149.5, and 224.4 corresponding to inorganic fluoride, and the C(1)–F and C(2)–F of excess inhibitor, respectively. In addition, a new resonance at δ 201.0 was assigned to an enzyme bound intermediate consistent with an α-anomeric configuration [30]. Further evidence supporting such an intermediate came from the ^{19}F NMR spectrum of the denatured inactivated enzyme, prepared by overnight dialysis in 8 M urea, which retained the peak ascribed to the E–I complex.

With the information obtained from these studies, Withers attempted to clarify the involvement of aspartic acid and glutamic acid residues in the catalytic mechanism of glycosidases [30,31]. Accordingly, incubation of [1-^{3}H]2′,4′-dinitrophenyl 2-deoxy-2-fluoro-β-D-glucopyranoside (**25**) with *Agrobacterium*β-glucosidase followed by peptide cleavage of the inactivated enzyme produced two radiolabeled

oligopeptides. These peptides were then subjected to Edman sequencing which identified two peptide chains: I–T–E–N–G–A and Y–I–T–E–N–G–A. This result is consistent with an inhibitor-enzyme adduct involving a glutamic acid since a "burst" of radioactivity was observed upon cleavage of this residue. Further sequence alignment revealed Glu358 to be the nucleophilic residue trapped by the inhibitor **25**.

2.4. UDP-N-acetylglucosamine enolpyruvyl transferase (MurZ)

The gene product of *MurZ*, UDP-Glc*N*Ac enolpyruvyl transferase, catalyzes the formation of enolpyruvyl-UDP-Glc*N*Ac (**26**) between the 3-OH of UDP-Glc*N*Ac (**27**) and the C(2)-position of phosphoenolpyruvate (PEP, **28**, Scheme 6). This reaction is the first committed step in the assembly of the bacterial peptidoglycan cell wall [32]. MurZ, along with 5-enolpyruvyl-shikimate-3-phosphate (EPSP) synthase, are the only known enzymes which catalyze the unusual transfer of an enolpyruvyl group to a co-substrate alcohol involving cleavage of the C–P bond of PEP (**28**). MurZ shows moderate sequence identity (~20%) to EPSP synthase, which catalyzes the attachment of PEP (**28**) to the 5-OH group of shikimate-3-phosphate via a single non-enzyme bound tetrahedral intermediate [33,34]. Despite this sequence identity, it was believed that catalysis by UDP-Glc*N*Ac enolpyruvyl transferase proceeded via a covalent enzyme-PEP adduct [35–37]. This apparent mechanistic divergence between these two enzymes prompted Walsh to further investigate the catalytic mechanism of MurZ.

Using the fluorinated PEP analogues, (*Z*)-fluorophosphoenolpyruvate [(*Z*)-FPEP, **29**] and (*E*)-fluorophosphoenolpyruvate [(*E*)-FPEP, **30**], Walsh was able to isolate and characterize two tetrahedral intermediates (**31** and **32**, Scheme 7) upon incubation with MurZ and UDP-Glc*N*Ac (**27**) that mirror the catalytic intermediates under normal catalysis (**34b** and **34a**, Scheme 8) [38]. However, their rates of formation are roughly 10^4 times slower than the analogous non-fluorinated substrates. Additionally, there was no breakdown of **32** in the forward reaction to the corresponding fluorinated enolpyruvyl-UDP-Glc*N*Ac under extended reaction times, which translates into a 10^6-fold rate reduction compared to normal catalysis accounting for

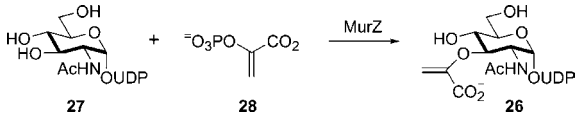

Scheme 6.

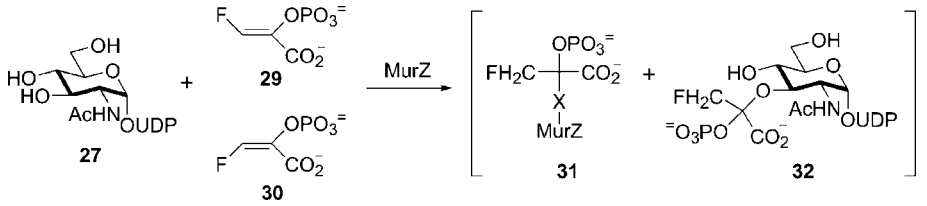

Scheme 7.

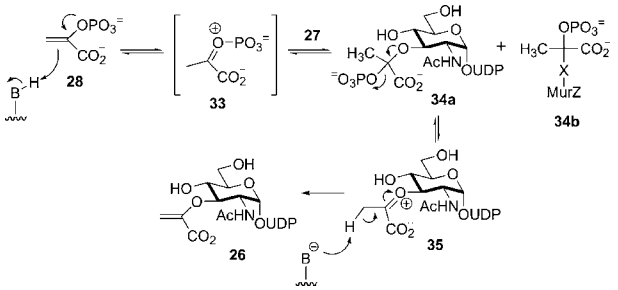

Scheme 8.

the observed enzyme inactivation. Interestingly, data gathered from rapid quench experiments showed that **32** and **31** are interconverted directly in the active site invoking no C–H bond cleavage and FPEP formation. More importantly, their results suggested that the enzyme adduct is derived from **34a**, and formation of **34b** is not required on the primary pathway for catalysis as originally surmised [35–37]. These kinetic data, along with similar results obtained from investigations of EPSP synthase, led Walsh to propose that the catalytic mechanism of MurZ involves the formation of two discrete oxocarbenium ion intermediates as shown in Scheme 8. Protonation of PEP (**28**) at the C(3)-position would result in the oxonium ion **33**, which is rapidly trapped by the C(3)–OH of UDP-Glc*N*Ac (**27**). Next, ionization of the phosphate group of the newly formed PEP-UDP-Glc*N*Ac adduct (**34a**) would result in a second oxonium ion intermediate **35**. Deprotonation of the now activated hydrogen on the methyl group, as a result of oxonium ion formation, leads to enolpyruvyl-UDP-Glc*N*Ac (**26**). The substitution of a fluorine for either vinylic hydrogen of PEP (**28**) would markedly destabilize the formation of an adjacent carbocation which explains the suppressed rate of catalysis for UDP-Glc*N*Ac enolpyruvyl transferase with fluorinated versions of phosphoenolpyruvate.

2.5. Thiamin phosphate synthase

Thiamin phosphate synthase catalyzes the penultimate step in the biosynthesis of vitamin B_1 (thiamin pyrophosphate) producing thiamin phosphate (**36**) from 4-amino-5-(hydroxymethyl)-2-methylpyrimidine pyrophosphate (HMP-PP, **37**) and 4-methyl-5-(β-hydroxyethyl)thiazole phosphate (Thz-P, **38**, Scheme 9) [39]. Thiamin pyrophosphate is an essential water-soluble vitamin necessary for the production of adenosine triphosphate (ATP), the main source of cellular energy in all organisms.

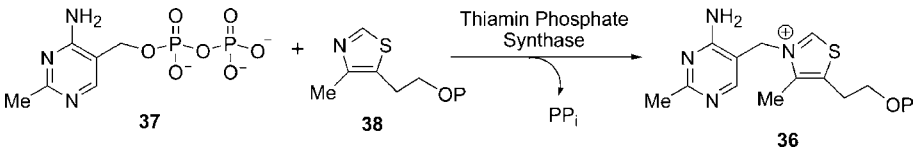

Scheme 9.

Since humans lack the biosynthetic machinery to produce vitamin B_1, the enzymes in the pathway have become attractive targets for the development of anti-microbial agents.

The reaction catalyzed by thiamin phosphate synthase could proceed by an associative (S_N2-like) process in which a concerted nucleophilic displacement of the pyrophosphate moiety of HMP-PP (**37**) by the thiazole nitrogen of Thz-P (**38**) leads directly to **36**. Alternatively, a dissociative (S_N1-like) process could also account for the formation of **36**. As shown in Scheme 10, ionization of the pyrophosphate group of HMP-PP (**37**) would afford the stabilized benzylic carbocation **39**, which is then trapped by the nucleophilic nitrogen of Thz-P (**38**) to furnish **36**.

To distinguish between the two proposed mechanisms, Begley conducted incubation studies with the C(2)-substituted analogues of HMP-PP (**40** and **41**, Fig. 4) [40]. If the reaction proceeds via a carbocation intermediate, then the reaction rate will be highly dependent upon the nature of the C(2)-substituent. For example, substitution of the methyl group in HMP-PP (**37**) with a trifluoromethyl group (CF_3-HMP-PP, **40**) or a methoxy group (MeO-HMP-PP, **41**) should result in a reduced reaction rate in the former case and an accelerated reaction rate in the latter case. On the other hand, the k_{cat} is not expected to be greatly affected if the reaction proceeds via an associative process.

Both CF_3-HMP-PP (**40**) and MeO-HMP-PP (**41**) were individually incubated with thiamine phosphate synthase and Thz-P (**38**), and the k_{cat} for each reaction was determined by a modified version of the thiochrome assay [40]. It was determined that the k_{cat} for CF_3-HMP-PP (**40**) was 7800 times lower than that for the natural substrate HMP-PP (**37**) while the k_{cat} for MeO-HMP-PP (**41**) was 2.8 times greater than that for HMP-PP (**37**). The extremely large perturbation in the reaction

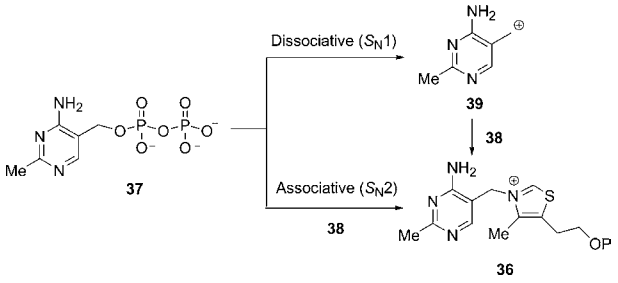

Scheme 10.

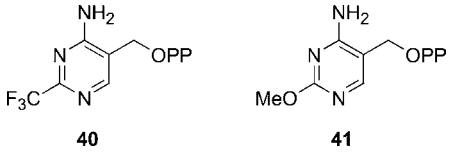

Fig. 4. Derivatives of 4-amino-5-(hydroxymethyl)-2-methylpyrimidine pyrophosphate.

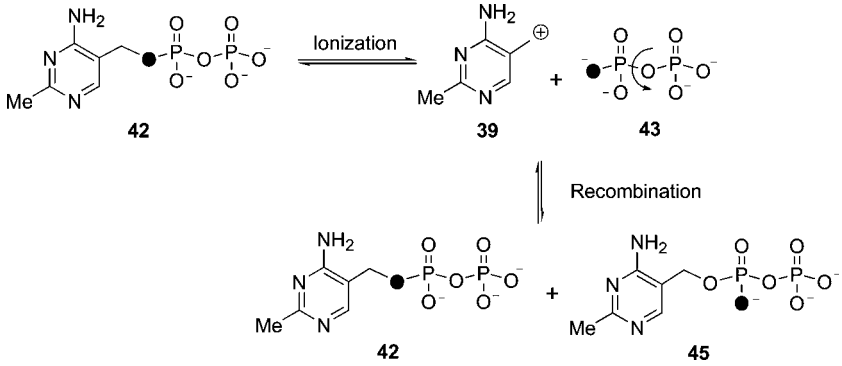

Fig. 5. Pathway for PIX utilizing [^{18}O]HMP-PP.

rate as a result of substitution of the methyl for a trifluoromethyl group is strongly suggestive of a carbocation intermediate. Additional evidence supporting the existence of a cationic transition state was obtained from the positional isotope exchange (PIX) experiment depicted in Fig. 5 [40].

Assuming the involvement of a carbocation intermediate in the thiamin phosphate synthase-catalyzed reaction, ionization of the pyrophosphate moiety of ^{18}O-labeled HMP-PP (**42**) would lead to the ion pair of **39** and **43**. Due to the free rotation of the P–O bond of **43**, recombination of the ion pair would result in scrambling of the ^{18}O-label, providing a mixture of **42** and **45**. As such, incubation of the ^{18}O-labeled HMP-PP (**42**) with thiamin phosphate synthase followed by dephosphorylation and hydrolysis of the pyrophosphate group by alkaline phosphatase resulted in an estimated 32% exchange of ^{16}O for ^{18}O in **42** (due to the co-production of **45**) as determined by GC/MS analysis. The observance of a positional isotope exchange further suggested that thiamin phosphate synthase proceeds by a dissociative mechanism.

2.6. *Cyclopropane fatty acid synthase*

Cyclopropane fatty acid (CFA) synthases catalyze the cyclopropanation of phospholipids such as 3-palmitoyl-2-oleoyl-phosphatidylethanolamine (POPE, **46**) in eubacteria. Cyclopropanation occurs at the olefinic side chain which typically resides some 9–11 carbon units from the ester linkage with *S*-adenosyl-L-methionine (SAM, **47**) serving as the methylene donor as outlined in Scheme 11. Cyclopropanated fatty acids (such as **48**) are involved in numerous cellular events such as protection of bacteria from environmental stress, alteration of membrane structural integrity, and overall virulence [41–45].

Several mechanisms have been proposed to account for the ring forming event and are depicted in Scheme 12. Mechanism A involves the formation of a corner-centered or a nonclassical delocalized carbocation intermediate (**50**) resulting from nucleophilic attack of *S*-adenosyl-L-methionine (**47**) by the isolated olefin of **46** [46–49]. In mechanism B, nucleophilic attack on SAM (**47**) is assisted by an enzyme

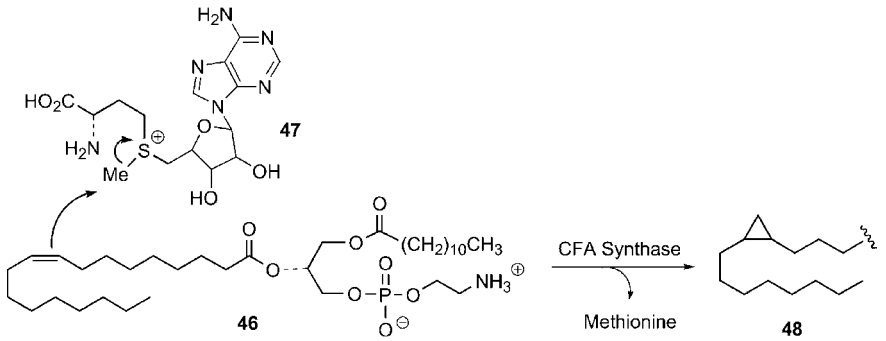

Scheme 11.

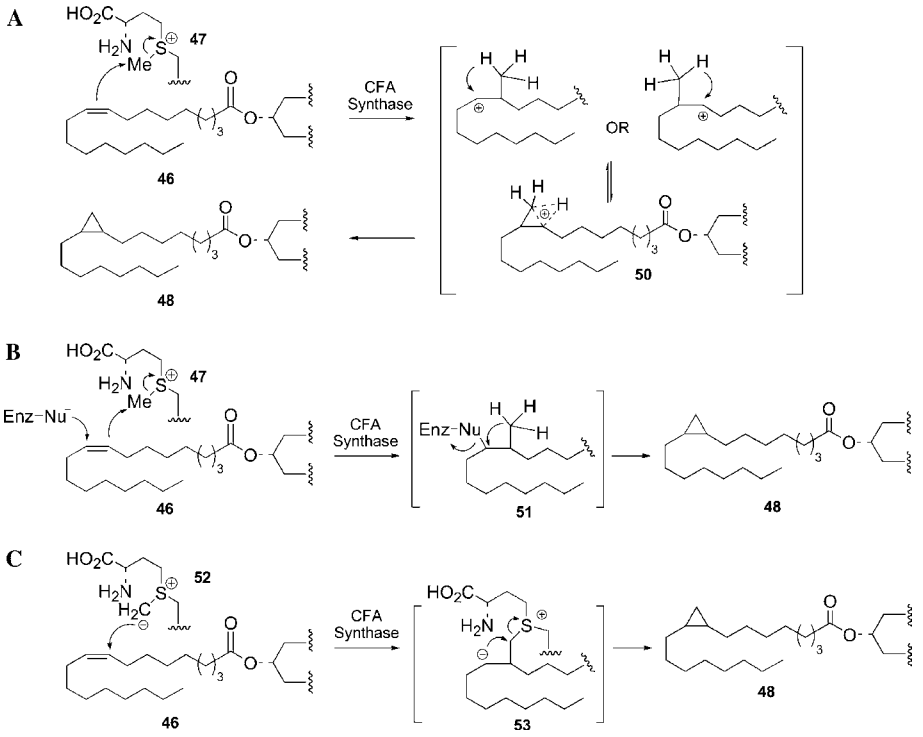

Scheme 12.

active site residue leading to the covalent adduct **51**. Decomposition of the covalent adduct **51**, which is initiated by proton abstraction of the seemingly unactivated methyl group, occurs during the ring closing step. A third possibility entails the deprotonation of SAM (**47**) to afford the corresponding sulfur ylide **52** [50]. Sulfur ylides of the type shown in mechanism C are not well-precendented in biological

systems. However, their use in natural products synthesis is commonplace making a route involving a sulfur ylide a possibility to be considered.

Investigations into the catalytic mechanism of cyclopropane fatty acid synthase from *Escherichia coli* have recently been conducted by Liu and co-workers [51]. To distinguish between the involvement of a cationic transition state (mechanism A, Scheme 12) or those with more anionic character (mechanisms B and C, Scheme 12), 3-palmitoyl-2-(9- and 10-fluorooleoyl)-phosphatidylethanolamine (PFOPE, **54** and **55**) and 3-palmitoyl-2-(9,10-epoxyoleoyl)-phosphatidylethanolamine (PEOPE, **56**) were synthesized as mechanistic probes (Fig. 6). PFOPE (**54** and **55**) contain a highly deactivated olefinic moiety, due to the electronegative nature of fluorine, and are expected to substantially increase the activation energy for a cationic process. As a result, if mechanism A is operative, a severely suppressed reaction rate should be observed (Scheme 13). Alternatively, in mechanism B, PFOPE (**54** and **55**) would be expected to cause either inactivation by direct β-elimination of the fluoride ion to form **65**, or by α-elimination of the fluoride ion followed by a 1,2-H shift of the generated carbene intermediate to give **66**, or turnover to the fluorocyclopropane **60** by the normal catalytic process. Similar inactivation or turnover can also be envisioned for mechanism C (Scheme 13). The exact pathway for turnover or inactivation would be dependent upon the regiochemistry of the nucleophilic addition. The electrophilic nature coupled with the intrinsic ring strain associated with epoxides make them susceptible to ring opening events. These properties led to the design of PEOPE (**56**), which was anticipated to form a covalent adduct with either the enzyme or SAM (**47**), if an anionic intermediate was present during catalysis by CFA synthase.

As it turned out, neither PFOPE (**54** and **55**) nor PEOPE (**56**) was a substrate for CFA synthase. Rather, both probes behaved as reversible inhibitors against the physiological substrate POPE (**46**). Incubation with PFOPE (**54** and **55**) led to a reduced catalytic efficiency (30–70%) while PEOPE (**56**) led to a nearly complete loss of enzyme activity (97%). The reduced turnover with PFOPE (**54** and **55**) is indicative of a carbocation mechanism. In addition, since neither PFOPE (**54** and **55**) or PEOPE (**56**) resulted in a covalent modification, a pathway involving nucleophilic attack may be ruled out. The near total loss of activity observed with PEOPE (**56**)

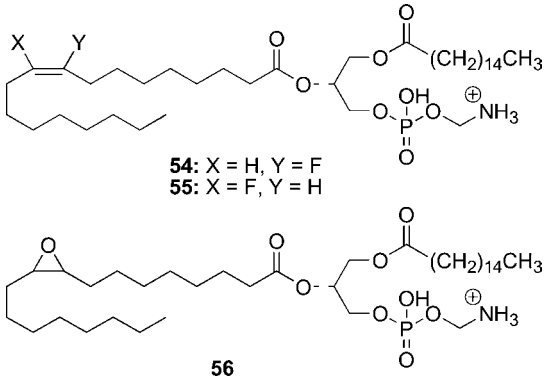

Fig. 6. Structures of mechanistic probes for CFA synthase.

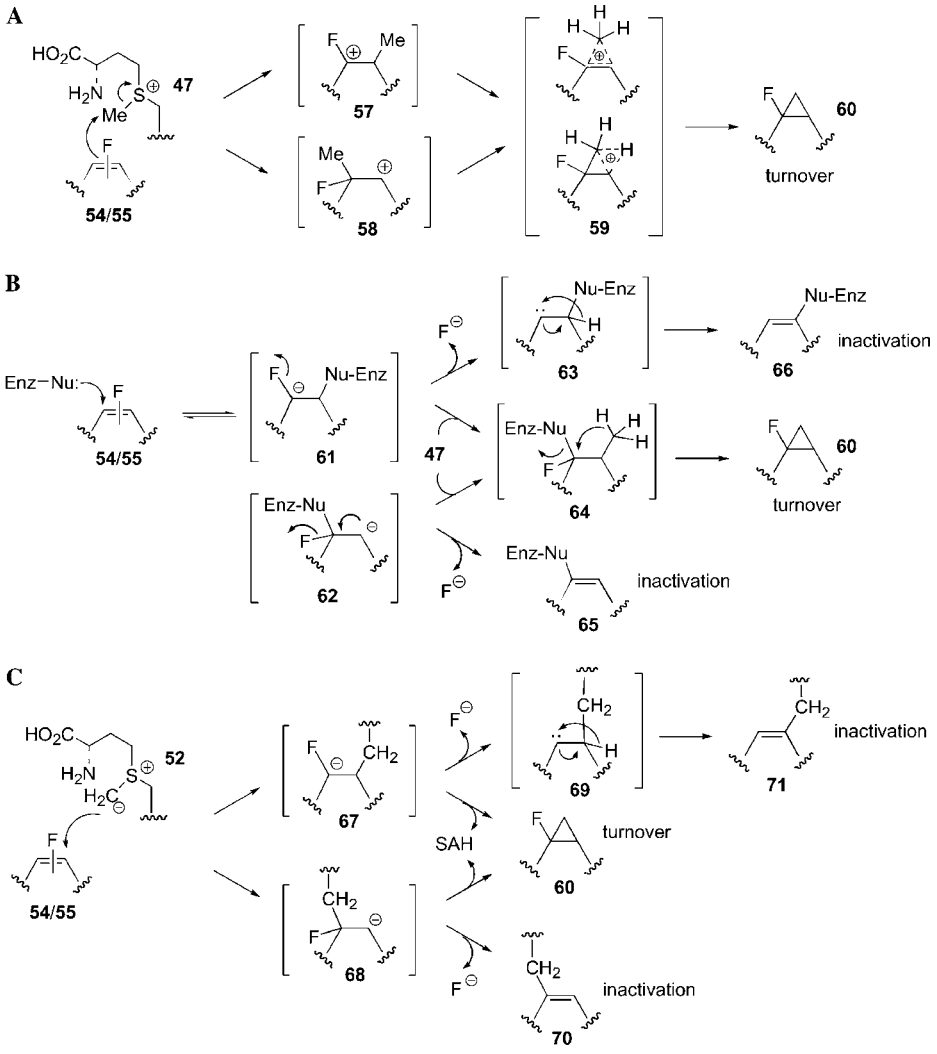

Scheme 13.

may merely be a reflection of favorable interactions of the epoxide moiety leading to increased binding affinity to the enzyme.

3. Oxidation/reduction mechanisms

3.1. Thymidylate synthase

The enzyme thymidylate synthase (TS) catalyzes a key step in DNA biosynthesis. It is responsible for the de novo production of thymidine-5′-phosphate (TMP, **72**)

from 2′-deoxyuridine-5′-phosphate (UMP, **73**) utilizing the coenzyme N^5,N^{10}-methylene-5,6,7,8-tetrahydrofolate ([CH_2]H_4folate, **74**) as seen in Scheme 14. The reaction constitutes a reductive methylation in the conversion of UMP (**73**) to TMP (**72**) with concomitant oxidation of [CH_2]H_4folate (**74**) to 7,8-dihydrofolate (H_2folate, **75**). The cofactor is subsequently regenerated by the combined action of dihydrofolate reductase and serine hydroxymethyltransferase. The key role of thymidylate synthase in the biosynthesis of DNA precursors has made it an attractive target for the design and development of chemotherapeutic agents to inhibit DNA synthesis.

Early mechanistic studies of the thymidylate synthase-catalyzed reaction revealed that the C(5)–H of UMP (**73**) exchanged with ^3H_2O at a rate approximately 80% the rate of H_2folate (**75**) formation, consistent with a secondary isotope effect involving a change in the hybridization state of C(5) from sp^2 to sp^3 during catalysis [52,53]. A turning point in the mechanistic studies of thymidylate synthase came from experiments using the fluorinated analogue [5-F]-2′-UMP (FUMP, **76**) by Santi et al. [54]. Incubation of enzyme and [CH_2]H_4-[^{3}H]folate with FUMP (**76**), led to the formation of a stable enzyme-[CH_2]H_4-[^{3}H]folate-FUMP adduct (**77**). The complex was stable to treatment with 6 M guanidine hydrochloride, providing preliminary evidence for the formation of a covalent bond between FUMP (**76**) and thymidylate synthase (Scheme 15). A decrease in the absorbance at 269 nm was observed indicating a

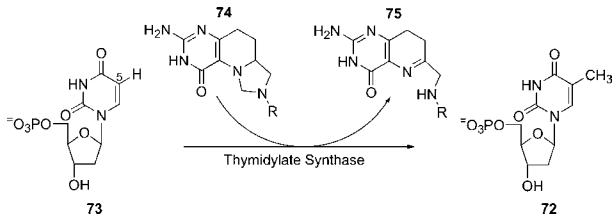

Scheme 14.

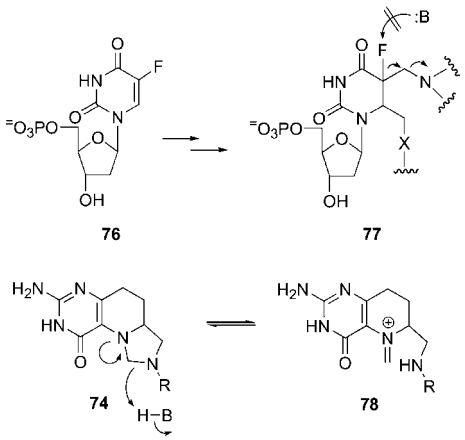

Scheme 15.

disruption of the π-system in the nucleotide moiety presumably at the C(5)–C(6) alkene. This decrease was accompanied by an increase in the absorption at 330 nm. This shift was attributed to a conversion of $[CH_2]H_4$folate (**74**) to the corresponding N^5-iminium ion **78**, as shown in Scheme 15. The iminium ion **78** has been postulated to be the actual reactive electrophilic species of methylation reactions mediated by $[CH_2]H_4$folate (**74**) [55,56]. Furthermore, use of [2-^{14}C]- and [6-^{3}H]FdUMP (**79**) gives a $k_H/k_T = 1.23$, which can be translated into a $k_H/k_D = 1.15$, and is indicative of a secondary isotope effect in the rehybridization of the C(6)-carbon from sp^3 to sp^2 during dissociation of the complex.

The data compliled from the experiments involving FUMP (**76**) led Santi et al. [54] to propose a mechanism for thymidylate synthase as shown in Scheme 16. First, nucleophilic attack by an active site residue onto the C(5)–C(6) alkene of UMP (**73**) would result in the covalent adduct **80**. This step would be consistent with the kinetic isotope effect results indicating a hybridization change from sp^2 to sp^3, and the prior model study demonstrating that the C(6)-position of UMP (**73**) is susceptible to nucleophilic attack [57,58]. Next, addition to the iminium ion **78** would furnish the ternary complex **81**. Formation of the ternary complex **81** was later unequivocally established from site-directed mutagenesis experiments involving the E60A and E60L mutants of thymidylate synthase from *Lactobacillus casei* [59].

The breakdown of the ternary complex **81** was first hypothesized to involve a [1,3] antarafacial shift of the C(6′)-H of the cofactor [60]. However, this type of rearrangement is not allowed by the Woodward–Hoffman rules for orbital symmetry. An alternative explanation for the transfer of the C(6′)–H from the coenzyme to the substrate would involve the formation of the exocyclic methylene **82** via deprotonation of the C(5)–H and elimination of the coenzyme [61]. A pathway involving this route would provide an explanation for the inhibitory effects of FUMP (**76**). Next, transfer of the C(6′)–H from the cofactor would afford the methyl group of TMP (**72**) consistent with previous isotope exchange experiments [62]. Preliminary evidence

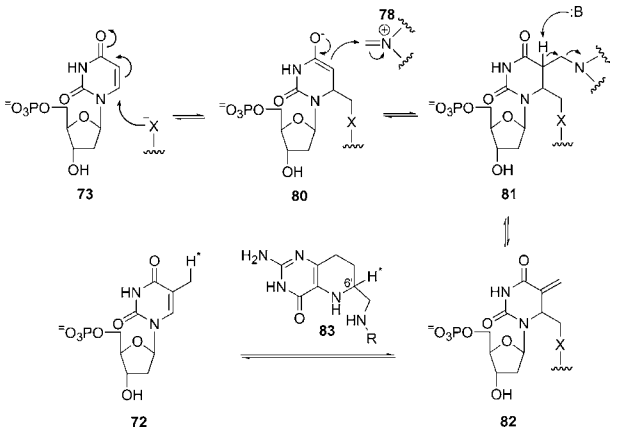

Scheme 16.

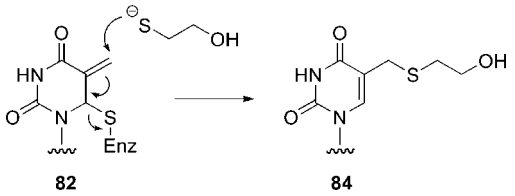

Scheme 17.

supporting this elimination/addition pathway involved the use of 5-(hydroxymethyl)uracil derivatives and studies of the enzyme 2′-deoxyuridylate hydroxymethylase [63]. Further proof for the presence of the exocyclic methylene intermediate **82** was provided by Schultz and co-workers [64] during their work on the kinetic analysis of unnatural amino acid mutants of thymidylate synthase containing tryptophan analogues at position 82. Schultz found that the W82Y mutant provided substantial amounts of a new product that was characterized as the β-mercaptoethanol adduct **84** of the exocyclic methylene intermediate **82** (Scheme 17). Since the adduct **84** cannot arise from a direct S_N2 substitution of intermediate **81** due to steric constraints within the enzyme active site, the likely precursor to **84** must be **82**, providing a complete picture for the mechanism of thymidylate synthase.

3.2. Estrogen synthetase (aromatase)

A critical juncture in steroid biosynthesis in humans is mediated by the enzyme estrogen synthetase (aromatase) which catalyzes the conversion of androstenedione (**85**) to estrone (**86**) in human placental microsomes as illustrated in Scheme 18. Aromatase is a P450 enzyme and consumes three equivalents of both NADPH and molecular oxygen (O_2) in the aromatization of the A-ring of androstenedione (**85**). Early mechanistic work determined that 19-hydroxyandrostenedione (**88**) and 19-oxoandrostenedione (**90**) are intermediates along the biosynthetic pathway towards estrone (**86**) [65]. Therefore, a mechanism involving sequential oxidations of the angular C(10)-β-methyl group of (**85**) appears plausible.

In attempts to regulate this important biological process, Robinson prepared 19-fluoroandrost-4-ene-3,17-dione (**91**) and 19,19-difluoroandrost-4-ene-3,17-dione (**92**)

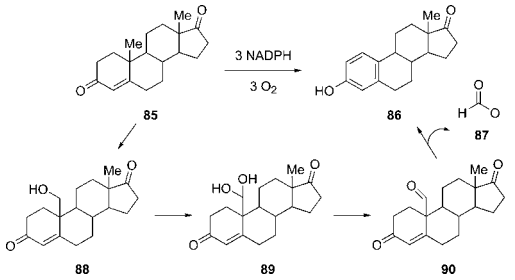

Scheme 18.

as mechanism-based inhibitors or probes [66]. They anticipated that processing of the fluorinated analogues by the normal catalytic cycle would result in the inactivation of the enzyme by modification of an active site residue as depicted in Scheme 19. For the monofluorinated derivative **91**, the initial oxidation was expected to provide the fluorohydrin **93** which would be subsequently processed to the *gem*-diol intermediate **94**. Decomposition of **94** could afford either the carboxylic acid **95** or the highly reactive acyl fluoride **96**. Following an analogous line of reasoning, the difluorinated analogue **92** would provide the same acyl fluoride intermediate **96** by expulsion of a fluoride ion after the initial oxidation step. Trapping an active site residue by **96** would lead to enzyme inactivation.

The monofluorinated analogue **91** turned out to be a competitive inhibitor for the enzyme with 50% inhibition when the enzyme and inhibitor ratio was about 1:3 [66]. Interestingly, incubation of **91** yielded estrone (**86**) as the only detectable product, as characterized by mass spectral analysis. Obviously, the formation of either **95** or **96** did not occur. This result can be rationalized by the expulsion of the fluoride leaving group following the initial oxidation (Scheme 20) to yield the aldehyde **90**, which is along the normal catalytic route for this enzyme.

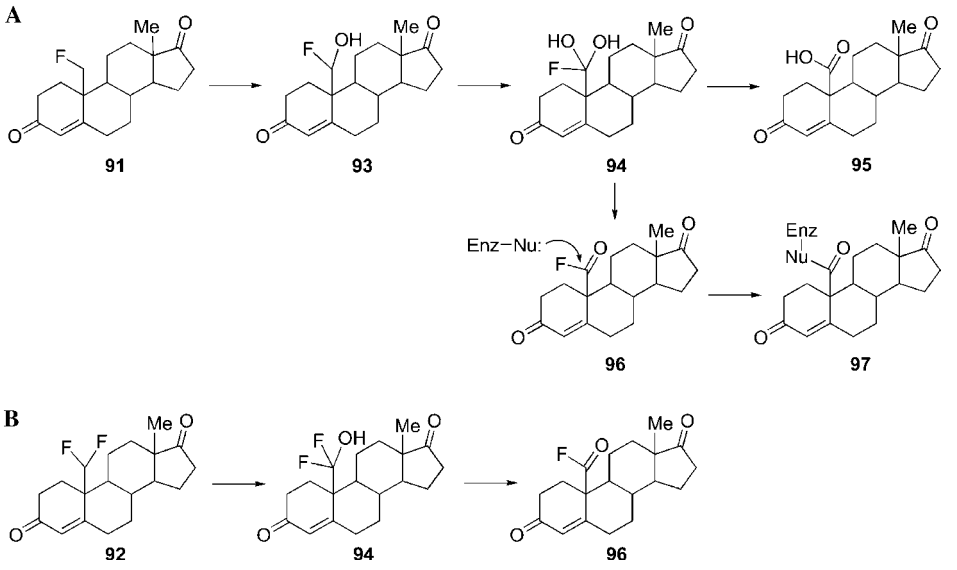

Scheme 19.

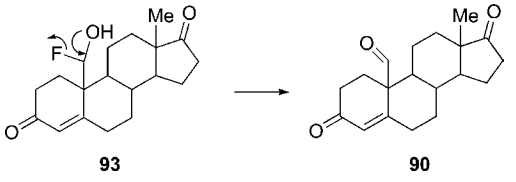

Scheme 20.

On the other hand, the difluorinated derivative **92** behaved as a time-dependent irreversible inhibitor of estrogen synthetase with a K_I = 1.0 μM and a k_{inact} = 0.023 min^{-1} [66]. The mode of inactivation was irreversible because enzyme activity could not be restored by extensive dialysis of the E–I complex, or by treatment of the reaction mixture with either dithiothreitol or ethanolamine hydrochloride. In addition, the rate of inactivation was significantly decreased in the absence of NADPH suggesting that oxidation of the substrate is a prerequisite for inhibition by **92**. Inactivation was likely due to the formation of the acyl fluoride **96** as shown in Scheme 19.

To confirm that inactivation was due to formation of the acyl fluoride **96**, synthetic **96** was prepared and incubated with the enzyme [66]. However, these studies were complicated due to the hydrolytic instability ($t_{1/2}$ = 14 min at 37 °C) of **96** in the buffer solution (10 mM potassium phosphate, 100 mM KCl, 1 mM EDTA). Nonetheless, preliminary rate studies indicated **96** is a reversible inhibitor of aromatase with 50% inhibition occurring at a concentration of 4 μM. In fact, 50% inhibition was the highest level obtained even when 10 μM inhibitor was used over a timeframe of 30 min. It was previously determined that all three oxidation steps occur at the same catalytic site without the release of any intermediates prior to estrone (**86**) [67]. In view of this observation, the failure of synthetic **96** to act as an irreversible inhibitor may be a reflection of its inability to enter the enzyme active site.

3.3. CDP-D-glucose 4,6-dehydratase (E_{od})

A common entry point in the biosynthesis of deoxysugars is the reaction catalyzed by glucose 4,6-dehydratase, involving a regiospecific C(4) oxidation of an NDP-glucose **98**, followed by deoxygenation of the C(6)–OH to provide the 4-keto-$\delta^{5,6}$-glucoseen intermediate (**100**, Scheme 21). The α,β-unsaturated ketone **100** is further processed to NDP-4-keto-6-deoxy-sugar **101** via reduction by NAD(P)H during the second phase of the catalytic cycle [68]. An example of this transformation is found in the enzyme CDP-D-glucose 4,6-dehydratase from *Yersinia pseudotuberculosis* [69]. The involvement of the enzyme bound NAD^+ coenzyme was found to be critical for enzyme activity. It was also demonstrated that the C(4)-hydrogen lost

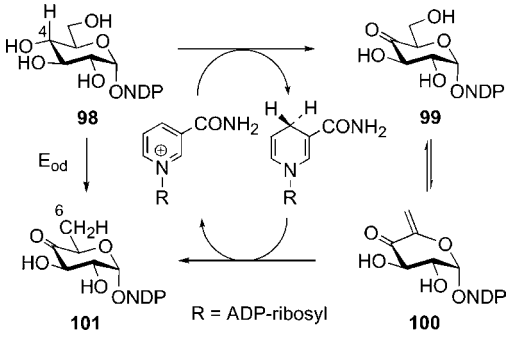

Scheme 21.

in the initial oxidation was returned to the C(6)-CH_3 group from labeling studies using (6*S*)- and (6*R*)-CDP-D-[4-^{2}H,6-^{3}H]glucose [70]. This intramolecular hydrogen migration is consistent with the mechanism depicted in Scheme 21 in which NAD^+ accepts a hydride during formation of the 4-keto sugar intermediate **99** and subsequently returns that hydride to the glucoseen intermediate **100** in a 1,4-addition.

To develop methods to control this important step in deoxysugar biosynthesis, Liu and co-workers synthesized the difluoroglucose derivative **102** as a mechanistic probe or inhibitor beginning with commercially available methyl-α-D-glucopyranoside [71]. The difluorinated sugar **102** was found to be a potent inhibitor of E_{od} with a $k_{inact} = 2.4 \times 10^{-2}$ min^{-1} and a $K_I = 0.94$ mM as calculated from a plot of $t_{1/2}$ versus $[I]^{-1}$. Extensive dialysis of the E–I complex failed to regenerate enzyme activity which is consistent with irreversible inhibition. The fact that addition of the natural substrate **98** protected the enzyme from inhibition suggested that **102** binds at the active site. Furthermore, no NADH could be detected spectrofluorimetrically at the end of the reaction. A peak resonating at δ −119.6 was observed in the ^{19}F NMR spectrum of the reaction mixture indicating that fluoride ion was released during inactivation. Mass spectral analysis of the E–I complex gave a molecular weight of 40,825 ± 1.7 Da per monomer which is consistent with the formation of a covalent adduct between E_{od} (MW = 40,280 ± 5.4 Da) and the difluoroglucose **102** (MW = 545 Da). Taken together, these findings point to a mechanism for inhibition as shown in Scheme 22.

Inhibition of E_{od} by **102** could begin with oxidation of the C(4)–OH followed by reductive elimination to form the Michael acceptor **106**. Since NAD^+ was regenerated, there is no hydride available in the enzyme active site for reduction of the glucoseen intermediate **106** as would occur during the normal catalytic cycle.

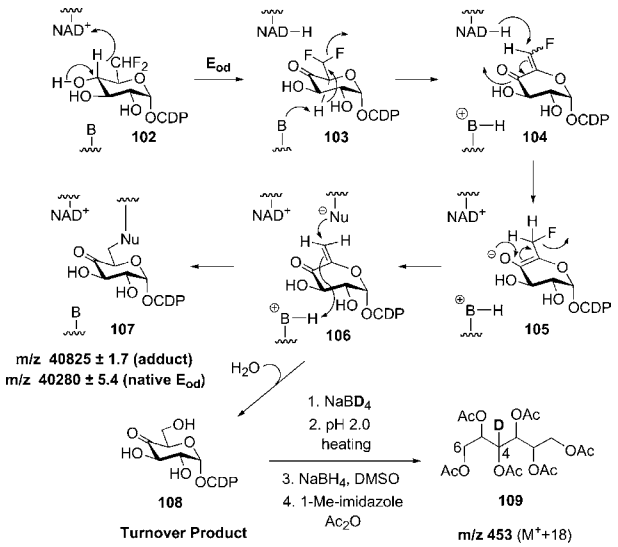

Scheme 22.

Instead, an active site residue is trapped by the α,β-unsaturated ketone leading to the covalent adduct **107**. Additional evidence in support of this mechanism came from the isolation of a turnover product that was identified as CDP-D-4-keto glucose (**108**) by the GC/MS assay shown in Scheme 22.

3.4. (S)-2-Hydroxypropylphosphonic acid epoxidase

(1*R*,2*S*)-Epoxypropylphosphonic acid (**110**), more commonly referred to as fosfomycin, is a clinically prescribed antibiotic for the treatment of both gram-negative and gram-positive bacteria. The biological target of fosfomycin is UDP-Glc*N*Ac-*O*-enolpyruvyl transferase (see Scheme 6), which catalyzes the first committed step in the biosynthesis of the peptidoglycan layer of the bacterial cell wall [32].

The penultimate precursor in the biosynthetic pathway of fosfomycin (**110**) has been identified as (*S*)-2-hydroxypropylphosphonic acid (HPP, **113**, Scheme 23) [72,73]. The conversion of HPP (**113**) into fosfomycin (**110**) is catalyzed by HPP epoxidase and constitutes a formal dehydrogenation of a secondary alcohol in establishing the oxiranyl ring system of fosfomycin (**110**). This proposal was confirmed by the formation of ^{18}O-labeled fosfomycin from ^{18}O-labeled HPP [74]. Since epoxidation reactions in biological systems typically involve the oxidation of an alkene by either heme-dependent cytochrome P450s or non-heme iron-dependent monooxygenases, the reaction catalyzed by HPP epoxidase via a dehydrogenation reaction of a 2° alcohol (HPP) is rather unusual [75]. The gene encoding HPP epoxidase from *Streptomyces wedmorensis* was recently subcloned and purified in its native form [74]. Subsequent biochemical studies revealed that the enzyme is a mononuclear non-heme iron-containing catalyst that is α-ketoglutarate independent. In addition, the enzyme consumes one equivalent of NADH in its production of one equivalent of fosfomycin using molecular oxygen (O_2) as the ultimate oxidant. The reaction also requires a reductase to serve as an electron shuttle, although other electron mediators such as FAD or FMN have been shown to be viable substitutes [74].

The observation that two products, fosfomycin (**110**) and 2-oxopropylphosphonic acid (OPPA, **114**), were produced in a 1:1 ratio upon incubation of racemic HPP with HPP epoxidase prompted Liu and co-workers [76] to undertake stereochemical investigations of the enzyme. As expected, the production of OPPA (**114**) was shown

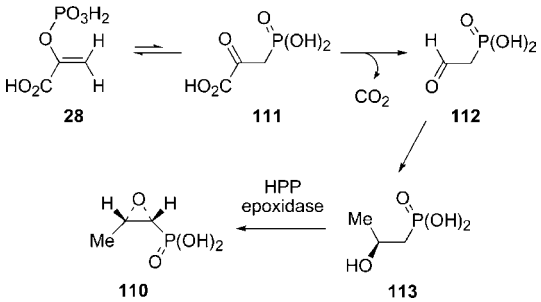

Scheme 23.

to originate from (*R*)-HPP (**115**) since it had previously been demonstrated that (*S*)-HPP (**113**) leads to fosfomycin (**110**) as shown in Scheme 23. The conversion of (*S*)-HPP (**113**) to fosfomycin (**110**) has been postulated to involve the formation of a reactive iron-oxo species **116** which undergoes homolytic fragmentation of the Fe–O bond to form **110** as outlined in Scheme 24. Similar pathways could also account for the formation of OPPA (**114**) in which formation of the α-radical **117** followed by β-hydrogen abstraction and tautomerization of the intermediate enol **118** would afford **114**. On the other hand, hydroxylation of the β-carbon would result in the *gem*-diol intermediate **119**, which could also explain the production of OPPA (**114**).

To probe the viability of these mechanistic proposals, Liu and coworkers [76] synthesized HPP containing a ^{13}C-label at the β-C ([2-^{13}C]HPP, **120**) as well as the 1,1-difluoro HPP analogue (**121**) as shown in Fig. 7. The [2-^{13}C]HPP (**120**) analogue was designed as a probe for the hydroxylation at the β-C as proposed in mechanism B, while the 1,1-difluoro derivative **121** was expected to behave as an inhibitor of HPP epoxidase if formation of an α-radical is a prerequisite for turnover to OPPA (**114**).

Incubation of racemic [2-^{13}C]HPP (**120**) under an ^{18}O atmosphere yielded OPPA (**114**) without any detectable ^{18}O incorporation as indicated by the absence of an isotopic shift in the ^{13}C NMR spectrum, thus invalidating a *gem*-diol intermediate such

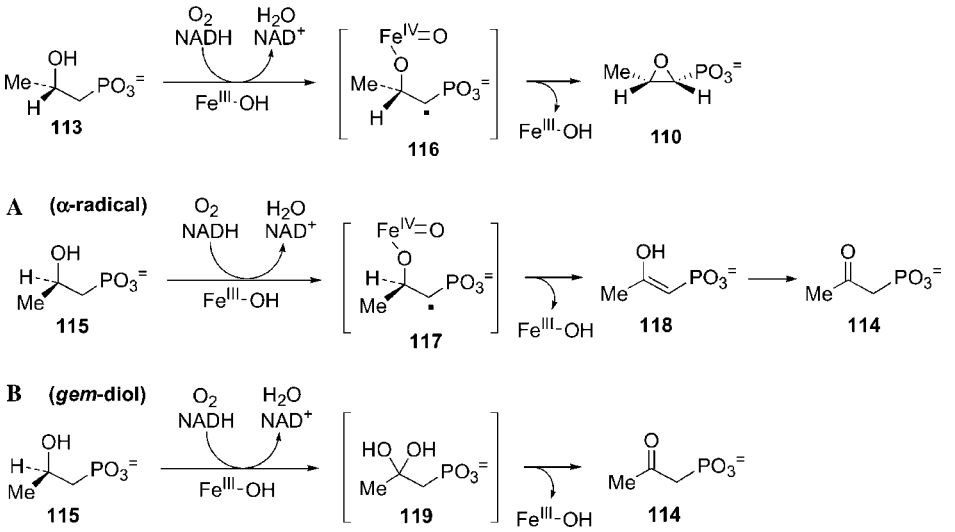

Scheme 24.

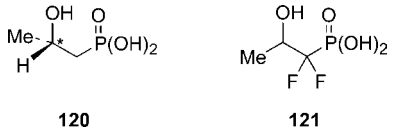

Fig. 7. Mechanistic probes for 2-oxopropylphosphonic acid formation.

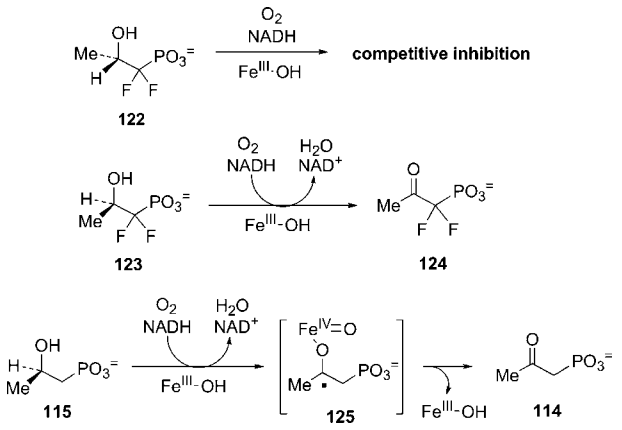

Scheme 25.

as **119** en route to **114**. Unexpectedly, incubation of racemic **121** resulted in partial loss of enzyme activity. Subsequent incubation experiments employing enantiomerically pure (*S*)-1,1-difluoro-HPP (**122**) and (*R*)-1,1-difluoro-HPP (**123**) (Scheme 25), obtained from a lipase resolution of the corresponding diethylphosphonic ester of HPP, revealed that (*S*)-**122** behaved as a tight binding inhibitor, consistent with the intermediacy of an α-radical in the formation of fosfomycin. However, (*R*)-**123** was converted to 1,1-difluoro-2-oxopropylphosphonic acid (**124**) at a rate (k_{cat}(**123**) = 162 ± 7 nmol mg^{-1} min^{-1}) comparable to that for the nonfluorinated substrate (k_{cat}(**115**) = 76 nmol mg^{-1} min^{-1}). The fact that **123** is processed to **124** rules out the possibility of an α-radical initiated pathway. In addition, the similar k_{cat} values for **123** and **115** do not support a carbocation intermediate since a substantially reduced turnover rate would have been anticipated for such a reaction pathway upon incubation of the 1,1-difluorinated analogues **121/123**.

The fact that **123** was accepted as a substrate and subsequently turned over by HPP epoxidase provides a wealth of information regarding the mechanism of OPPA (**114**) formation. An alternative pathway for formation of OPPA (**114**) is shown in Scheme 25 in which formation of the ketyl radical **125** is the presumptive first step in the conversion of (*R*)-**115** to **114** followed by homolytic cleavage of the Fe–O bond.

3.5. TDP-L-rhamnose synthase

Oxidation–reduction processes are ubiquitous in biological systems. These redox events are frequently mediated by pyridine nucleotides such as NAD(P)$^+$ or NAD(P)H. These coenzymes serve as electron shuttle systems by either accepting or donating an electron pair according to the requirements of the enzyme. One of the more common transformations involving these cofactors is the interconversion of a ketone and hydroxy group. Interestingly, few investigations have examined the regioselectivity of this reduction process. This is due in part to the fact that only

a single reaction pathway exists wherein the hydride is delivered to the ketone bearing carbon due to the polarity of the carbonyl functional group.

In an attempt to develop mechanism-based inhibitors for TDP-L-rhamnose synthase (RfbD), which catalyzes the reaction (**126** → **127**) shown in Scheme 26, the difluorinated analogue **128** was synthesized from L-rhamnose to evaluate its inhibitory effect on RfbD and to probe the regiospecificity of pyridine nucleotide hydride transfer reactions [77].

The comparable electronegativities between fluorine and oxygen as well as the ability of fluorine to participate in hydrogen bonding suggested that **128** would be a suitable substrate mimic. Two routes for inhibition were considered (Scheme 27). Processing of **128** by the normal catalytic pathway would result in formation of the carbanion intermediate **132**. However, the formation of a carbanion at the *gem* difluorocarbon is unfavorable due to electrostatic repulsion between the anionic center and the electron pair of the fluorine atom. This repulsion could be alleviated by α-elimination of fluoride to produce the reactive carbene intermediate **133**, which could then inactivate the enzyme by reacting with an active site residue. Alternatively, if hydride transfer occurred with the opposite regioselectivity, a doubly stabilized carbanion **129** would be generated and subsequent β-elimination of a fluoride ion would generate the reactive alkene **130**. The vinylfluorinated alkene **130** could then inactivate the enzyme by covalent modification of an active-site residue.

Incubation of **128** with RfbD, a NADH-dependent dehydrogenase which has been demonstrated to transfer the 4′-H_s of NADH to reduce **126**, did not result in enzyme inactivation [77]. Instead, the difluorinated derivative **128** was a substrate, albeit a poor one, with a $k_{cat} = 12.7 \pm 3.8$ min^{-1} (k_{cat}(**126**) = 258.3 ± 25.0 min^{-1})

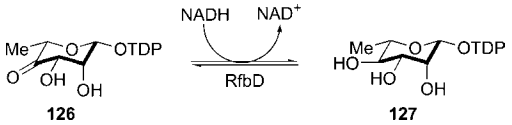

Scheme 26.

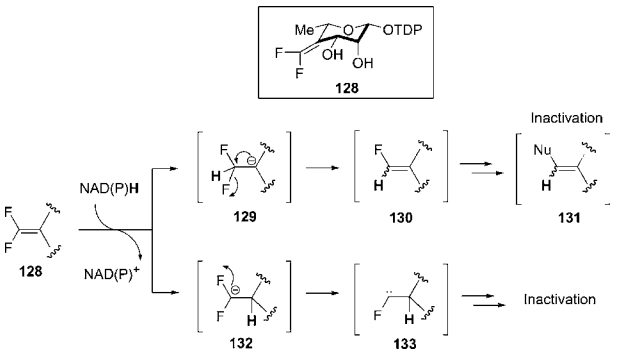

Scheme 27.

and a $K_m = 40.1 \pm 17.0$ mM (K_m(**126**) = 0.30 ± 0.03 mM). The ^{19}F NMR spectrum of the reaction mixture displayed a resonance at δ −119.9. This observation, reflecting the presence of a fluoride ion, is indicative of the cleavage of a C–F bond during catalysis. Using a previously established GC/MS protocol [78], the turnover products from incubation of **128** with RfbD in the presence of [4′*S*-^{2}H]NADH were identified as the tetraacetates **134**, **135**, and **136** (Scheme 28). The mass spectra for the C(4) containing fragments of **135** and **136** revealed shifts of one and two mass units, respectively. These shifts are characteristic of deuterium incorporation from [4′*S*-^{2}H]NADH onto the terminal carbon of the exocyclic difluoromethylene moiety as illustrated in Scheme 28.

The observed reversed regioselectivity can be explained by two mechanisms. One involves the formation of carbene intermediates (**142/144**) followed by a rearrangement involving a 1,2-H shift. This mechanistic proposal is theoretically sound and would represent a rare example implicating the intermediacy of a carbene species in an enzyme reaction. However, these results are also consistent with a second mechanism in which the hydride addition to the difluoromethylene moiety occurs at the difluorinated end (**137**), opposite from the site predicted on the basis of the reduction of a normal keto functional group. Such a regioselectivity is well

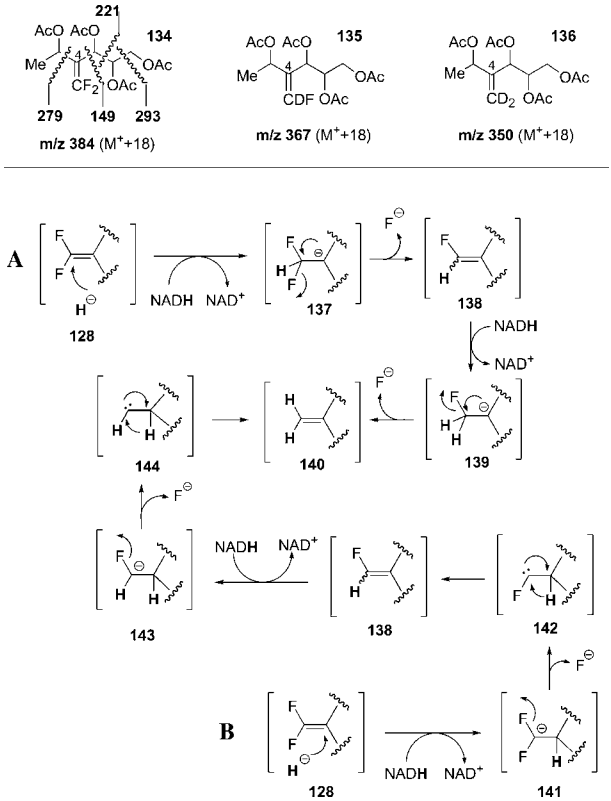

Scheme 28.

precedented in chemical models because nucleophilic addition to fluoroalkenes prefers a route in which the number of fluorines β to the electron rich carbon in the transition state is maximized. In this mechanism, the difluoromethylene group may be regarded as a carbonyl mimic with reversed polarity in enzyme catalysis. While further experiments are needed to discriminate between these mechanistic possibilities, these results suggest that the apparent regioselectivity of hydride transfer in a pyridine nucleotide dependent enzyme can be changed by altering the electrochemical properties of the reaction center. Since the regioselectivity of most enzymatic reductions is governed by the binding of substrate within the active site, the fact that electronic alterations may affect the regiospecificity of hydride transfer from pyridine nucleotide cofactors may have relevance for the design of mechanistic probes and inhibitors for other enzyme classes.

4. Radical mechanisms

4.1. Chorismate synthase

Chorismate synthase is the seventh enzyme in the shikimate biosynthetic pathway and is responsible for the conversion of 5-enolpyruvylshikimate 3-phosphate (EPSP, **145**) to chorismate (**146**, Scheme 29). Further enzymatic processing of chorismate generates various primary and secondary metabolic building blocks including the aromatic amino acids phenylalanine, tyrosine, and tryptophan. The reaction catalyzed by chorismate synthase is formally a *trans*-1,4-elimination of the C(6)-*pro*-R hydrogen and the C(3)-phosphate group. However, concerted 1,4-eliminations have repeatedly been shown to follow a *cis*-1,4-elimination pathway [79,80]. In addition, reduced FMN is required for catalysis despite the fact that there is no net redox change [81]. These observations, along with the fact that chorismate synthase is present in bacteria and plants but not in mammals, has fueled interest in the elucidation of the enzyme mechanism so that novel chemotherapeutic agents can be designed.

Five mechanisms have been proposed to account for this intriguing transformation and are summarized in Scheme 30. An early proposal by Floss suggested a concerted E2-like elimination of the C(3)-phosphate group by a hypothetical active site residue, to form the covalent adduct **147** as depicted in mechanism A [82]. Subsequent removal of the C(6)-hydrogen would release the amino acid with concomitant formation of chorismate (**146**). In theory, the hypothetical residue could be the C_{4a} or N_5 position of the flavin cofactor which would explain the necessity of reduced FMN during catalysis. Mechanism B, proposed by Ganem in 1978, involves a

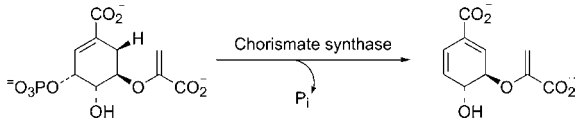

145 146

Scheme 29.

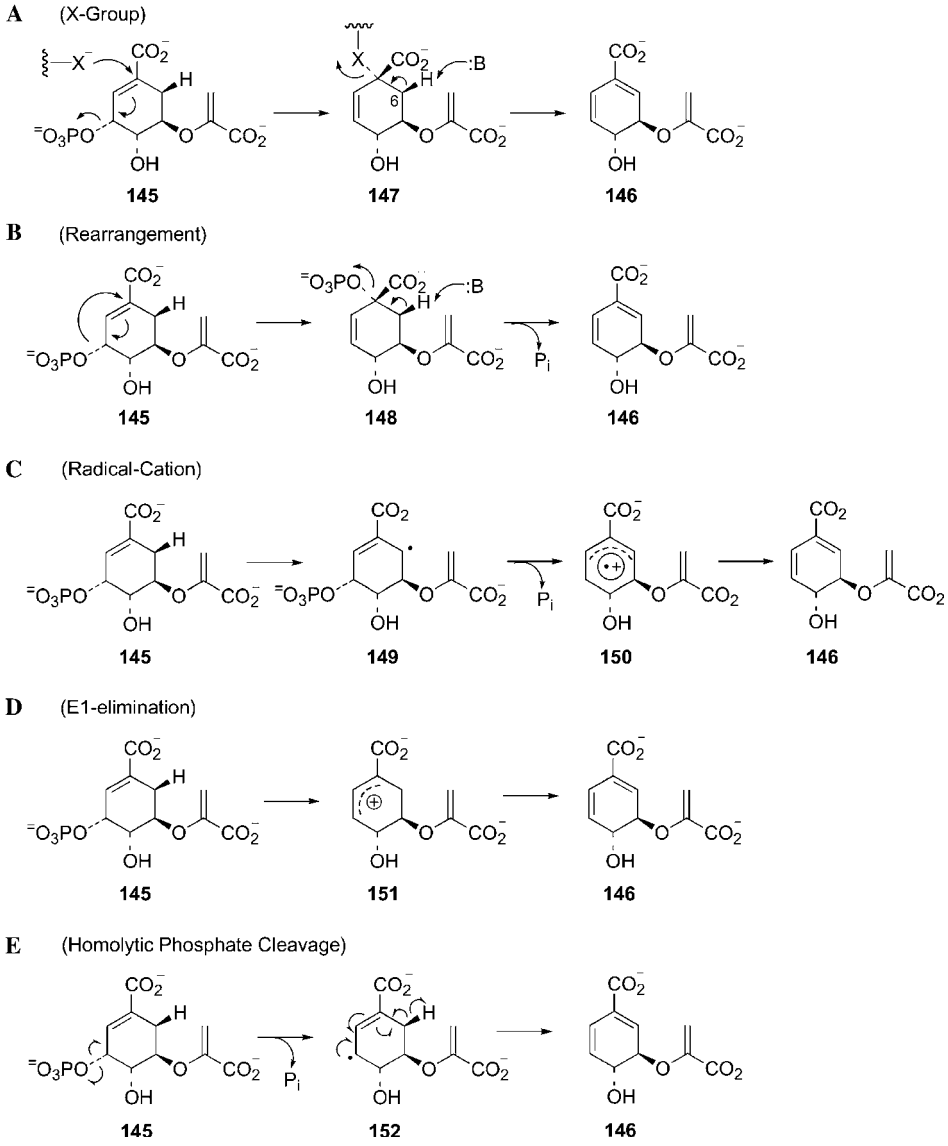

Scheme 30.

suprafacial 3,3-rearrangement of EPSP (**145**) to furnish the allylic phosphate isomer **148**, which then undergoes a *trans*-1,2-elimination to afford **146** [83]. While these types of sigmatropic rearrangements have precedence in the enzymatic cyclizations of geranyl and farnesyl pyrophosphates, such an allylic rearrangement pathway offers no obvious role for the requirement of a reduced FMN cofactor [84–87]. Alternatively, Bartlett proposed that hydrogen atom abstraction at C(6) occurs first to

provide the stabilized allyl radical **149**. Next, ionization of the C(3)-phosphate group would afford the transient radical cation **150**, as illustrated in mechanism C [88]. The ability of such radical intermediates to lower the activation energy and assist the ionization of allylic leaving groups has been demonstrated by MNDOC calculations and observed experimentally in related systems [89,90]. Single electron transfer from the flavin cofactor to the radical cation **150** would then afford chorismate (**146**). A route involving E1 elimination of the C(3)-phosphate group followed by deprotonation of the C(6)-hydrogen must also be considered (mechanism D). The role of reduced FMN in mechanism D may be stabilization of the allylic cation formed during catalysis. More recently, Bornemann proposed that homolytic cleavage of the C(3)-phosphate facilitated by reduced FMN is the presumptive first step in the reaction catalyzed by chorismate synthase. This results in the allyl radical **152**, which undergoes further oxidation to chorismate (**146**) via loss of a hydrogen radical from the C(6)-position (mechanism E) [91].

In 1986, Bartlett conducted incubation studies with "iso-EPSP" (**148**, Scheme 30), with purified chorismate synthase from *Neurospora crassa* [92]. If mechanism B was operative, then **148** should be processed by the enzyme to chorismate (**146**). However, Bartlett found that **148** was not a competent substrate for the enzyme-catalyzed reaction but in fact was a competitive inhibitor with a binding affinity comparable to that of the natural substrate EPSP (**145**): K_i(**148**) = 8.7 μM, K_m(**145**) = 2.7 μM. This result is not consistent with the intermediacy of **148** during the enzymatic reaction.

Preliminary evidence supporting mechanisms C and D came from independent incubation experiments with (6*S*)-6-F-EPSP (**153**) with the enzyme from *E. coli* and the (*Z*)-fluoropyruvyl EPSP analogue (**154**, Fig. 8) with the enzyme from *N. crassa* [95,96]. Since both mechanisms C and D invoke a cationic intermediate, the presence of a fluorine substituent would be expected to decrease the overall rate of reaction. The (*Z*)-fluoropyruvyl EPSP analogue (**154**) was found to be a very poor substrate for chorismate synthase with a K_i = 13 μM and a V_{rel} approximately 2% that of EPSP (**145**) [95]. However, since the fluorine substituent in the EPSP analogue **154** resides in the side chain and not the cyclohexene core, it is not obvious how it is responsible for the decreased reaction rate. Incubation of (6*S*)-6-F-EPSP (**153**) displayed a more dramatic drop in the rate of reaction on the order of 270–370 times that of EPSP (**145**) [96]. Both of these results appeared to implicate the existence of a cationic intermediate in the conversion of EPSP (**145**) to chorismate (**146**). However, the lack of a "phosphate burst" upon incubation of **145** with chorismate synthase argues against a purely E1 mechanism. At the same time, these results ruled out a concerted E2-like elimination as proposed in mechanism A, since the

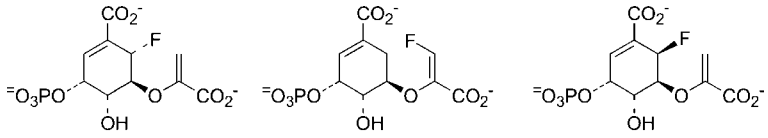

Fig. 8. Fluorinated analogues fo 5-enolpyruvylshikimate 3-phosphate.

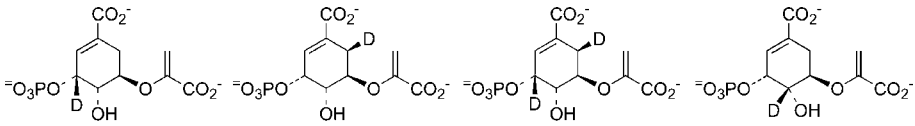

Fig. 9. Deuterated EPSP analogues for kinetic isotope exchange studies.

incorporation of a fluorine substituent at the C(6)-position would be anticipated to accelerate the rate of reaction.

Further evidence in support of mechanisms C, D, and E came from single and multiple turnover anaerobic stopped-flow experiments of the natural substrate **145** in the presence of recombinant *E. coli* chorismate synthase, $FMNH_2$, and $Na_2S_2O_4$ (required to reduce FMN to $FMNH_2$) [93]. Those experiments revealed the direct involvement of the flavin cofactor in catalysis as either a charge complex or a covalent flavin adduct as indicated by transient changes in the absorbance at 400 nm. However, the exact nature of the flavin cofactor remained elusive until incubation studies were performed with the EPSP analogue (6*R*)-6-F-EPSP (**155**, Fig. 8) [94]. Those investigations revealed an absorbance at 582 nm, which is consistent with the presence of a protein-bound flavin semiquinone free radical as a mixture of both anionic and neutral forms. While this absorbance was absent in incubation studies performed with **145**, the authors proposed that a free radical could be a transient intermediate that does not significantly accumulate when the C(6)-*pro*-R hydrogen is available for abstraction. These stopped-flow data, coupled with the observation that the enzyme is unable to process EPSP (**145**) to chorismate (**146**) in the presence of reduced 5-deaza-FMN, firmly established a direct role for the flavin coenzyme in the formation of a radical intermediate in catalysis [95].

Kinetic isotope effect studies have also been conducted using the EPSP analogues (**156**–**159**) shown in Fig. 9 [96,97]. While some conclusions have been drawn in favor of initial cleavage of the C(3)–O bond in the catalysis by chorismate synthase, definitive judgments cannot be made concerning the order of bond breaking in the transition state to distinguish mechanisms C, D, or E, because the values of the kinetic isotope effects are close to unity.

While the reaction mechanism of chorismate synthase remains somewhat ambiguous, it is clear that the use of fluorinated analogues of 5-enolpyruvylshikimate 3-phosphate (**153**–**155**) were instrumental in determining a role for the strict requirement for reduced FMN in catalysis. This finding allowed for the revision of mechanistic proposals and the design of further experiments to support or debunk them. Perhaps the future use of other fluorinated derivatives may prove useful in elucidating the mechanism of this mechanistically fascinating enzyme.

4.2. CDP-6-deoxy-L-threo-D-glycero-4-hexulose-3-dehydrase (E_1)/CDP-6-deoxy-L-threo-D-glycero-4-hexulose-3- dehydrase reductase (E_3)

3,6-Dideoxyhexoses are the major antigenic determinants found in the *O*-specific side chains of cell wall lipopolysaccharides of various gram-negative bacteria.

Studies aimed at understanding the biosynthesis of these carbohydrate residues in *Y. pseudotuberculosis* revealed an unusual enzymatic redox process for the deoxygenation of the C(3)-hydroxyl group of a 4-keto-6-deoxyhexose (**161**) to make the corresponding 4-keto-3,6-dideoxyhexose product (**160**) [98–104]. This intriguing C–O bond cleavage event is catalyzed by two enzymes: CDP-6-deoxy-L-*threo*-D-*glycero*-4-hexulose-3-dehydrase (E_1), a PMP/[2Fe–2S]-containing homodimeric enzyme, and CDP-6-deoxy-L-*threo*-D-*glycero*-4-hexulose-3-dehydrase reductase (E_3), a NADH dependent [2Fe–2S]-containing flavoenzyme. The cooperativity of E_1 and E_3 was established based on both in vitro and in vivo experiments [102]. Since [Fe–S] clusters are often invoked as one-electron carriers, the mechanism for this transformation was believed to involve a radical intermediate. As such, three mechanistic routes were proposed to explain the formation of **160** from CDP-6-deoxy-4-hexulose (**161**, Schemes 31–33) [101].

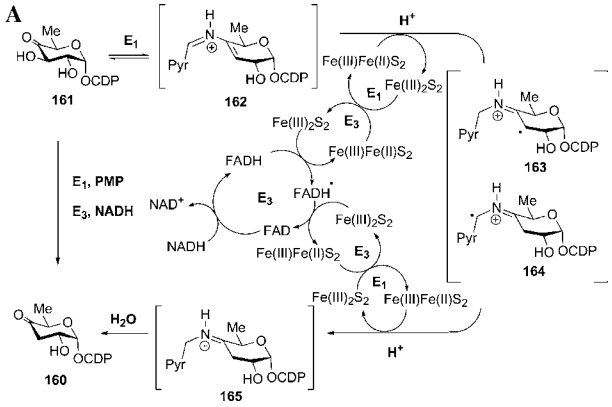

Scheme 31.

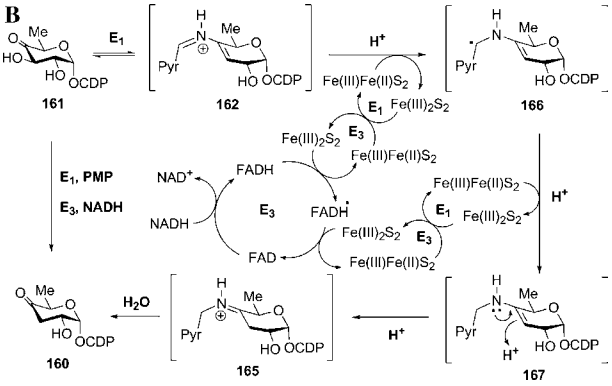

Scheme 32.

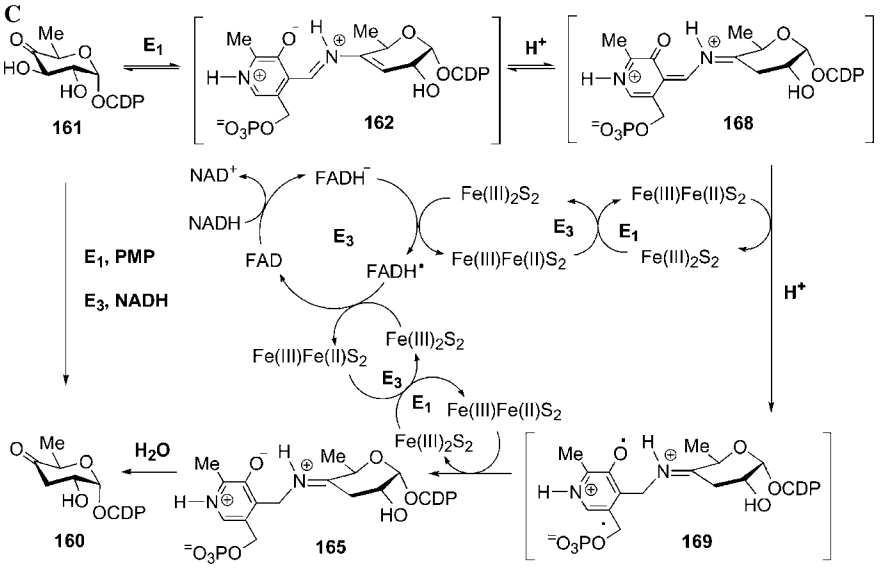

Scheme 33.

All three mechanisms implicate a role for the PMP coenzyme in E_1 in the reversible dehydration of the CDP-6-deoxy-4-hexulose intermediate (**161**) by conventional coenzyme B_6 chemistry [105,106]. However, they differ in the manner by which the PMP cofactor is regenerated. In mechanism A, single electron transfer from the [2Fe–2S] cluster in a 1,4-fashion could lead to either the C(3)-carbohydrate radical **163**, reminiscent of ribonucleotide reductase, or the benzylic radical **164** which has precedence in the PLP-conjugated radical found in the reaction catalyzed by lysine 2,3-aminomutase [107,108]. Mechanism B follows a similar course postulating a 1,2-addition to the iminium ion to form the benzylic radical at the 4′-position of the PMP cofactor **166**. Alternatively, as illustrated in mechanism C, tautomerization of the C(3′)-hydroxyl group on the PMP cofactor would furnish the corresponding quinone methide intermediate **168**, which upon single electron transfer from the [2Fe–2S] cluster of E_1 would afford the phenoxy radical intermediate **169**.

Several lines of evidence have been collected showing the formation of a flavin semiquinone radical during the catalysis [109]. The EPR studies of the half-reaction catalyzed by E_1 also revealed the transient formation of a substrate radical with its unpaired electron spin located mainly on the PMP coenzyme [101,109]. The kinetic properties of the substrate radical intermediate were also characterized by stop-flow spectrophotometry and rapid freeze quench EPR spectroscopy [109]. To provide further evidence in support of a PMP-based radical during the E_1/E_3-catalyzed deoxygenation reaction, the deuterated PMP analogues [2′-$^2H_3$]PMP (**170**) and [4′,5′-$^2H_4$]PMP (**171**, Fig. 10) were synthesized based on previously developed methodology [103,110].

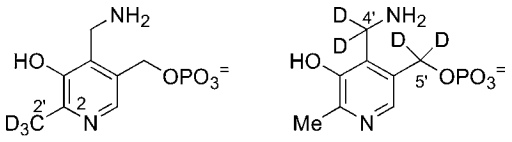

170 **171**

Fig. 10. Deuterated PMP analogues for CW EPR and ENDOR studies.

Reconstitution of apo-E_1 was accomplished with both labeled PMP derivatives **170** and **171** for use in CW EPR and pulsed electron nuclear double resonance (ENDOR) experiments. The CW EPR spectrum of E_1 reconstituted with **171** displayed a signal narrowed by approximately 3 G compared to a standard spectrum taken with unlabeled PMP [104]. This sharpening of the EPR signal is due to the substitution of hyperfine-coupled ^1H by ^2H, and reflects the close proximity between the unpaired electron spin and the ^2H substituents [111,112].

The ENDOR spectrum of **170** possesses at least one signal attributed to a ^2H nucleus at 3.2 MHz with a ^2H hyperfine coupling constant of 1.9 MHz, which translates into a ^1H coupling of approximately 12 MHz. Reconstitution of E_1 with **171** produced an ENDOR spectrum with a major peak at 4.1 MHz, correlating to a coupling constant of 3.7 MHz. In addition, multiple hyperfine couplings were observed perhaps reflecting inequivalent ^2H couplings from the 4′- and/or 5′-^2H of **171**. As further evidence in support of an organic radical residing on the PMP coenzyme, a Mims ENDOR difference spectrum [113] was obtained by substracting the [2′-$^2H_3$]PMP signals from the unlabeled PMP spectrum. As expected, the previously observed 12 MHz coupling seen for **170** was not present in the difference spectrum while a ^1H coupling of 7 MHz was detected corresponding to the methyl group in the unlabeled PMP.

While CW EPR and ENDOR spectroscopy aided in establishing the localization of an unpaired electron spin on the PMP coenzyme, the process of radical formation remained in question. To gain further insight into the feasibility of a phenoxy radical being generated on the PMP cofactor, the fluorinated PMP analogue (F-PMP, **172**, Scheme 34) was synthesized and incubated with E_1/E_3, NADH, and substrate [103]. The substitution of the 3′-OH with a fluorine was designed to prevent the tautomerization to the quinone methide intermediate **168**, thus inhibiting single electron transfer from the [2Fe–2S] cluster and, consequently, the formation of the phenoxy radical postulated in mechanism C.

Results of the incubation of F-PMP (**172**) are illustrated in Scheme 34. A GC/MS assay was able to detect the peracetylated alditols from the positive control in which PMP was added to the reaction mixture. However, when the enzyme was reconstituted with F-PMP (**172**), no product formation was observed [103]. At first glance, this result would suggest that the tautomerization step was inhibited preventing the stepwise electron reduction of the dehydration product **174**. However, since the reaction catalyzed by E_1/E_3 can be considered as two half-reactions, it is not clear at this juncture whether F-PMP (**172**) is inhibiting the reversible dehydration cata-

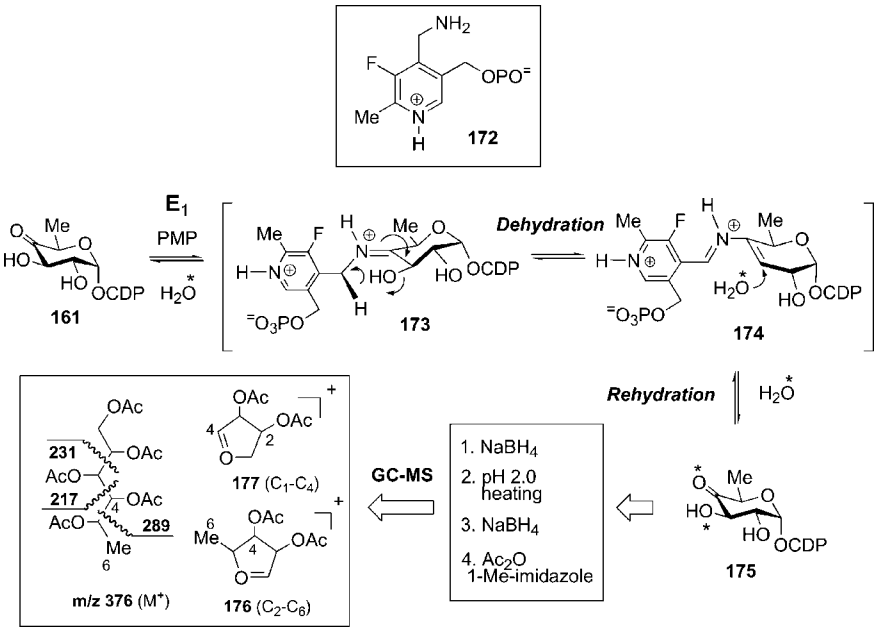

Scheme 34.

lyzed by E_1 or the stepwise electron transfer catalyzed by E_3. To determine whether F-PMP (**172**) was a competent coenzyme for the initial dehydration catalyzed by E_1, a series of incubation reactions was conducted in buffer prepared with $H_2{}^{18}O$. The isolated substrate (**175**) was then analyzed. The MS fragments containing the C(4)-oxygen linkage (such as **176**, **177**) were all shifted by two mass units due to ^{18}O exchange with the C(4)-ketone. However, fragments containing the C(3)-oxygen linkage were only shifted in a similar fashion due to re-hydration when PMP was added to the incubation mixture and not when F-PMP (**172**) was used. This clearly indicates that F-PMP (**172**) did not catalyze the reversible dehydration mediated by E_1. It was subsequently determined that E_1 reconstituted with F-PMP (**172**) was unable to abstract the C(4′)–H of the cofactor necessary for expulsion of the C(3)–OH group during catalysis [103].

The failure of F-PMP (**172**) to serve as a competent coenzyme may be due to the lowering of the pK_a of N-1, consequently, causing interruption of a salt bridge/hydrogen bonding network of N-1 with Asp199. Similarly conserved aspartates have been shown to be critical for activity in other PLP/PMP enzymes from site-directed mutagenesis experiments. While no further insight into the reaction catalyzed by E_1/E_3 was obtained with **172**, the use of F-PMP (**172**) did illustrate the importance of the C(3)–OH of PMP in catalysis and may reflect a general dependence of PLP/PMP-catalyzed reactions on the electronic nature of the coenzyme.

5. Stereochemical models/rearrangement mechanisms

5.1. CDP-D-tyvelose 2-epimerase

CDP-D-tyvelose 2-epimerase is responsible for the conversion of the 3,6-dideoxy sugar paratose (**178**) into tyvelose (**179**) via epimerization at the C(2)-position (Scheme 35) [114]. A fascinating feature of this NADH-dependent enzyme is its ability to catalyze epimerization at an unactivated carbon center. In most cases, sugar epimerases exert their effects at centers adjacent to a keto functionality which increases the acidity of the α-protons. This increase in acidity is often enough to allow a pair of enzyme active site bases to abstract the α-hydrogen and reprotonate the same carbon from the opposite face to result in epimerization.

Four possible routes have been postulated for this unusual process and are shown in Scheme 36 [114,115]. In mechanism A, which is reminiscent of UDP-galactose-4-epimerase [116–120], oxidation of the C(2)–OH would provide the corresponding C(2)–ketone **180**. Rotation of the hexulose around the P_β of UDP and the glycosyl oxygen (O_1) bond followed by NADH reduction would afford tyvelose (**179**). Mechanism B also invokes the NAD^+-mediated oxidation of the C(2)–OH to provide the C(2)-keto sugar **180**. Next, deprotonation of a C(3)–H would afford the enol **181** which could undergo reprotonation on the *re*-face to furnish **179**. The key feature of mechanism C is the reversible dehydration of the C(2)–OH as a result of oxidation of the C(4)–OH. Michael addition of H_2O from the solvent would result in **179**. Mechanism D is predicated on a retro-aldol fragmentation resulting in cleavage of the C(2)–C(3) bond followed by recyclization and reduction of the ensuing C(4)-ketone functional group to afford tyvelose (**179**).

A set of experiments were carried out to differentiate between the four mechanistic proposals in Scheme 36 [115]. First, incubation of CDP-paratose (**178**) and the epimerase in $H^{18}O$ revealed no incorporation of ^{18}O, thereby ruling out a dehydration/rehydration pathway (mechanism C). Second, incubation of enzyme with CDP-[2-$^2H_1$]paratose (**186**) did not result in deuterium incorporation at the C(3)-position of tyvelose (**179**) as predicted based on an intramolecular hydrogen migration route involving NAD^+/NADH (mechanism B). The remaining epimerization pathways were distinguished by incubation studies with CDP-[4-F]paratose (**187**, Fig. 11). Since a requisite of mechanism D is oxidation of the C(4)–OH to the corresponding ketone **182**, **187** should behave as an inhibitor of the enzyme if mechanism D is correct. In contrast, if mechanism A is operative, **187** is expected to be processed by the enzyme.

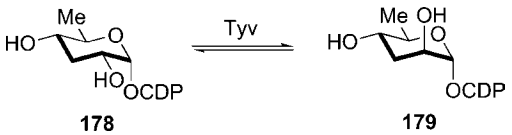

178 **179**

Scheme 35.

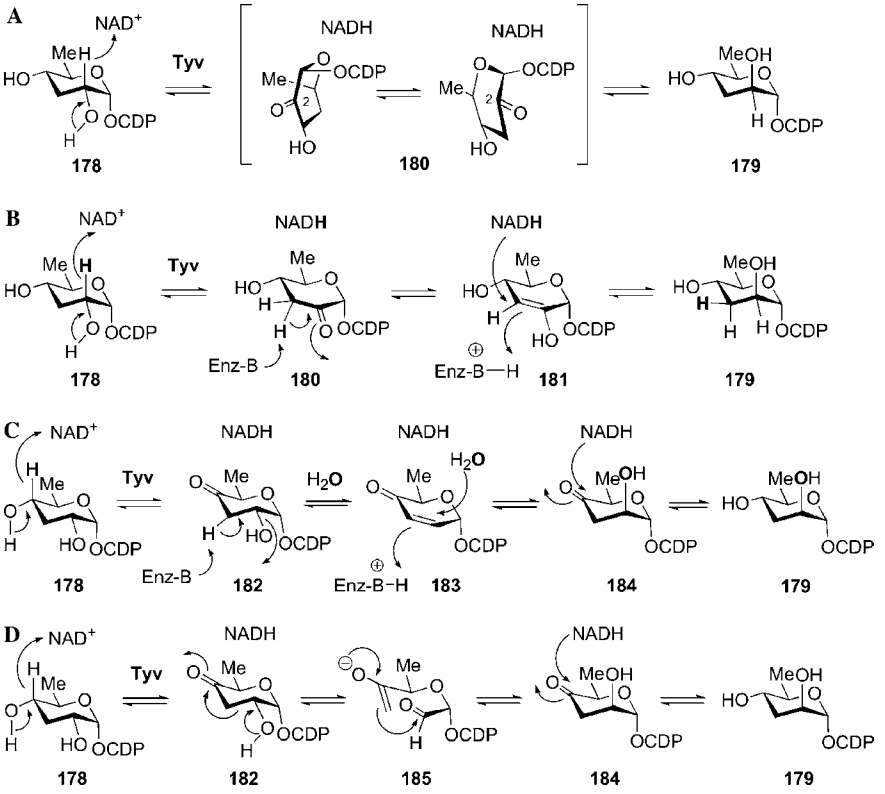

Scheme 36.

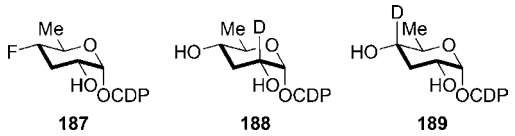

Fig. 11. Fluorinated and deuterated analogues of CDP-D-tyvelose 2-epimerase.

When **187** was included in the assay mixture, it functioned as a substrate with a $K_m = 42 \pm 2$ μM and a $k_{cat} = 0.7 \pm 0.1$ min^{-1} [115]. This result clearly argued against a retro-aldol process (mechanism D) leaving only mechanism A as the likely pathway. To directly probe the feasibility of mechanism A as the actual mode of action of CDP-D-tyvelose 2-epimerase (Tyv), an experiment is to determine the regiochemistry of the initial oxidation. This experiment was designed based on an observation that upon prolonged incubation with CDP-D-tyvelose epimerase with a 10-fold excess of CDP-paratose (**178**), NADH accumulated in the reaction mixture. Since C-2 oxidation is a pre-requisite for mechanism A, an analysis of deuterium incorporation into NADH after incubation of the C(2)- (**188**) or C(4)-deuterated (**189**)

CDP-paratose derivatives (Fig. 11) would provide unambiguous evidence to distinguish mechanism A from mechanism D. The results showed that only the nicotinamide coenzyme isolated from the incubation of the C(2)-labeled substrate contained deuterium. These findings firmly establish that the reaction catalyzed by CDP-D-tyvelose 2-epimerase is initiated by oxidation at C-2, followed by the transfer of the hydride from the transiently formed NADH to the opposite side of the 2-hexulose intermediate (**180**).

5.2. YerE

Yersiniose A (**190**) is an immunodominant sugar found in the *O*-antigen of *Y. pseudotuberculosis* VI [121]. YerE is a thiamin pyrophosphate (TPP, **191**) dependent flavoenzyme that catalyzes the attachment of a two-carbon chain from pyruvate (**192**) to CDP-4-keto-3,6-dideoxyglucose (**195**) to give **197**, which is the immediate precursor of yersiniose A (**190**, Scheme 37). The catalytic mechanism of YerE is believed to follow the standard TPP coenzyme chemistry beginning with nucleophilic attack of the thiazolium ylide (**191**) at the C(2)-position of pyruvate (**192**). Decarboxylation of the TPP adduct (**193**) would generate the stabilized carbanion **194** which undergoes 1,2-addition to the C(4)-keto group of **195**. Breakdown of the tetrahedral intermediate **196** would then produce yersiniose A (**190**) following NADPH-mediated reduction of the methyl ketone of **197**. The role of the flavin coenzyme is currently unknown but is not believed to be involved in catalysis, since reduction of YerE with sodium dithionite did not affect the enzyme's activity [121].

To develop methods for controlling this enzymatic reaction, the *exo*-difluoromethylene analogue **198** was synthesized [122]. The difluoromethylene moiety has been

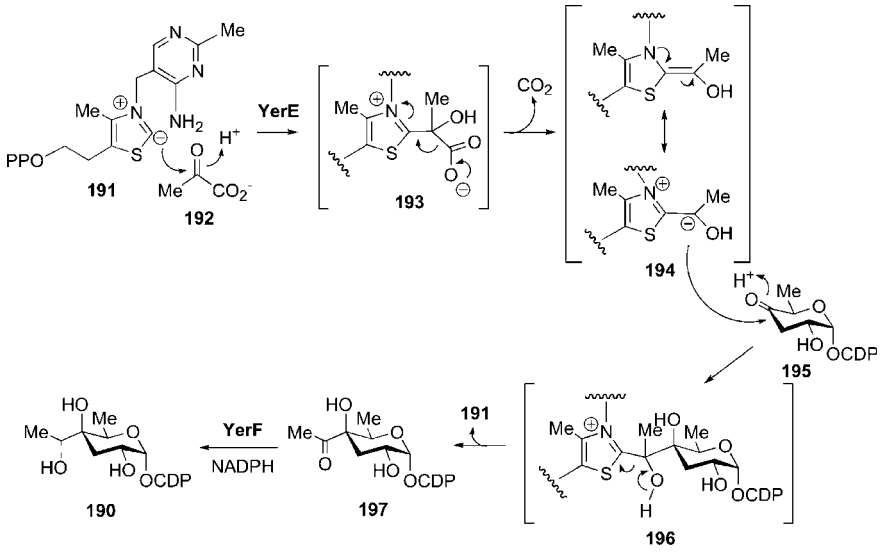

Scheme 37.

successfully utilized as a bioisostere for the carbonyl functional group [77] and it was believed that nucleophilic attack by the TPP ylide (**194**) would result in the corresponding tetrahedral intermediate **199** as illustrated in Scheme 38. At this juncture, two different pathways could be envisioned. Pathway A follows the same route as normal catalysis to give **200**. In pathway B, expulsion of a fluoride ion would turn over the monofluorinated sugar derivative **201** and the acetylated TPP (**202**), the latter of which may cause enzyme inactivation by trapping of an active site residue to yield the covalent adduct **203**.

Since nucleophilic additions to 1,1-difluoroolefins usually occur at the terminal methylene carbon, the mechanism shown in Scheme 39 should also be considered. Should this route be operative, then the first intermediate would be the adduct **204**, which could be turned over by protonation of the generated C(4)-carbanion to afford **205**. Inactivation of the enzyme from **204** could also occur via β-elimination of a fluoride ion to give **206**. When the TPP cofactor is regenerated from **206**, the resulting product **207** would be an excellent Michael acceptor with the potential to trap an active site nucleophile and covalently modify the enzyme (**208**).

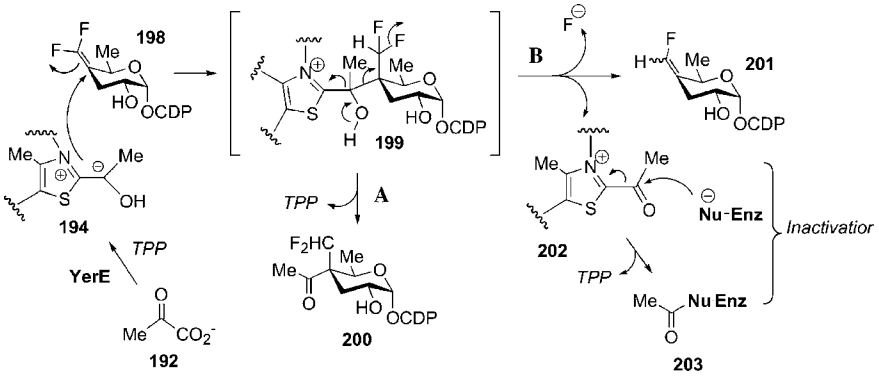

Scheme 38.

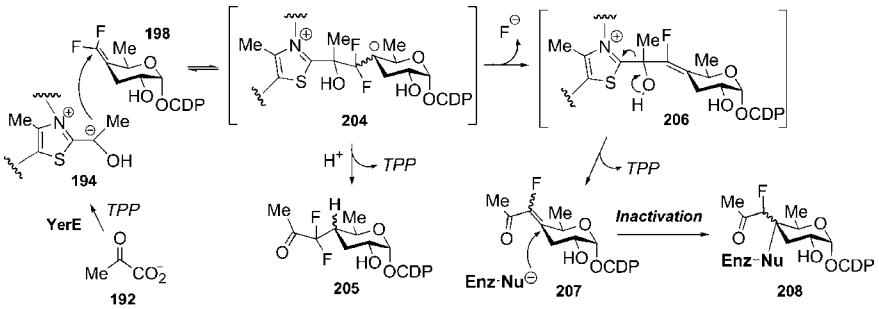

Scheme 39.

Unfortunately, incubation of the *exo*-difluoromethylene derivative **198** with YerE displayed no apparent effect on the enzyme activity [122]. It was not possible to detect the release of fluoride ion or the formation of any new products by HPLC analysis. This result was interpreted as an indication of the inflexibility of the enzyme active site of YerE to accommodate the extra steric bulk of the difluoromethylene moiety. While obviously disappointing, the design strategy described above should prove useful for elucidating the mechanisms of other enzymes which may be more accommodating of fluorinated substrate analogues.

5.3. UDP-galactopyranose mutase

The furanose form of galactose is prevalent in the surface polymers of microorganisms such as bacterial *O*-antigens, mycobacterial cell walls, fungal glycoconjugates, and protozoal cell membranes [123–125]. The biosynthesis of galactofuranose (**209**) originates from UDP-glucose (**210**) by the enzymatic action of UDP-galactose 4-epimerase followed by UDP-galactopyranose mutase (UDP-Gal*p* mutase) as shown in Scheme 40. UDP-Gal*p* mutase has attracted much attention in recent years not only for its biological importance, but also because of its intriguing mechanism, especially due to the observation that the reduced flavin plays a direct role in this transformation.

UDP-Gal*p* mutase contains a noncovalently bound flavin adenine dinucleotide (FAD) cofactor and catalyzes the transformation of UDP-galactose (**211**) to UDP-galactofuranose (**209**) via a formal ring contraction process. The requirement for a flavin cofactor during catalysis has sparked interest in elucidating the mechanism for this intriguing rearrangement. Several possible mechanisms have been proposed as illustrated in Schemes 41 and 42. In Scheme 41, oxidation of either the C(2)- or C(3)–OH, mediated by FAD, would facilitate cleavage of the C(1)–C(2) bond via a retro-Michael process (**214** → **215**) [126]. Michael addition of the C(4)–OH to the enone moiety of intermediate **216** would provide the ring contracted enediol **217**. Reduction by FADH would then regenerate the FAD coenzyme with concomitant formation of UDP-galactofuranose (**209**). Alternatively, cleavage of the anomeric C–O bond would result in the oxonium ion **221** (pathway A, Scheme 42). The distorted conformation of this highly reactive intermediate would allow for intramolecular attack of the C(4)–OH onto the anomeric carbon to furnish the bicyclic acetal **222**, which may also be generated via pathway B in a direct displacement reaction. Next, ring opening by an enzyme active site residue (**223**, pathway C) or by departure of the C(5)–OH to the oxonium ion **224** (pathway D), followed by rebound of UDP would furnish UDP-galactofuranose (**209**) [127].

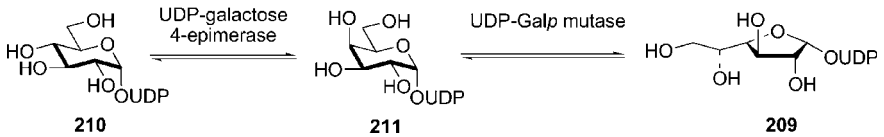

Scheme 40.

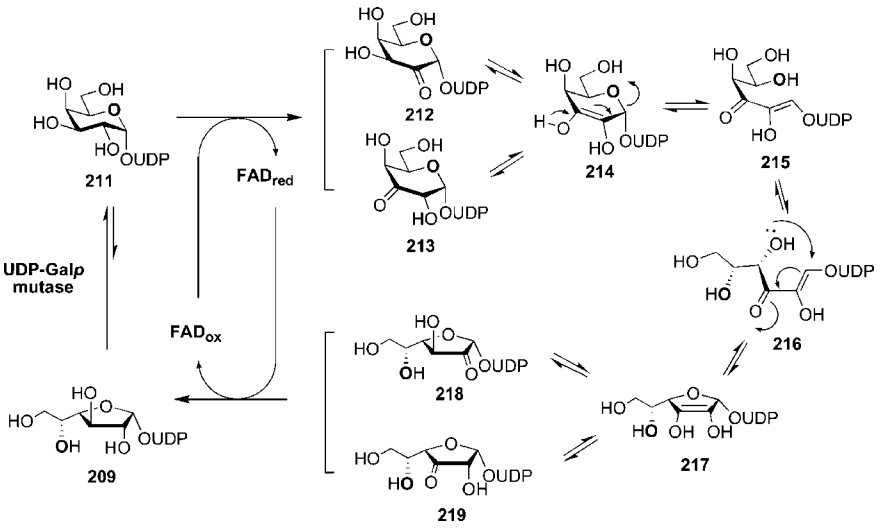

Scheme 41.

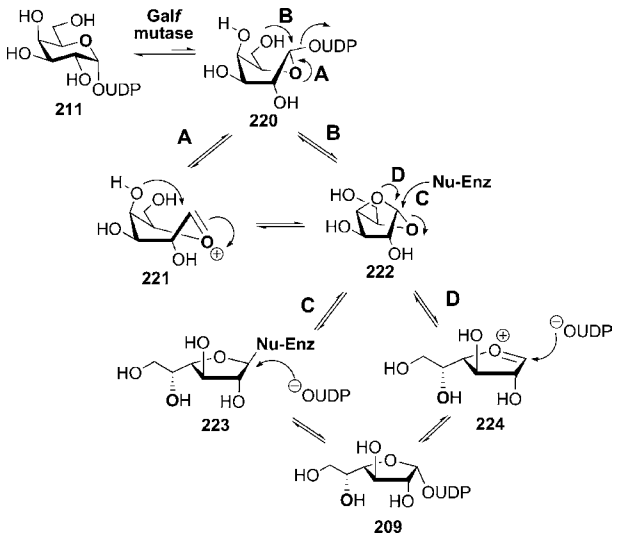

Scheme 42.

Studies by Blanchard involving doubly labeled [1-^{13}C, 1-^{18}O]UDP-galactose revealed that reversible cleavage of the anomeric C–O bond occurred during catalysis through observation of a positional isotope exchange at C-1, providing evidence for the mechanism shown in Scheme 42 [127]. Shortly thereafter, it was discovered that the flavin coenzyme was intimately involved in catalysis as indicated by an observed

rate enhancement (29 times higher) upon photoreduction of FAD in the presence of 5-deazariboflavin under anaerobic conditions [128]. One possible reason for the increased turnover of UDP-Gal*p* mutase in the presence of reduced flavin is the stabilization of the resulting oxonium ion intermediates **221**/**224** formed during catalysis by the reduced coenzyme [128].

To obtain further insight into the mechanism catalyzed by UDP-Gal*p* mutase, Liu and co-workers synthesized UDP-[2-F]Gal*f* (**225**) and UDP-[3-F]Gal*f* (**226**, Fig. 12) [126]. To facilitate kinetic determinations, the furanose forms were chosen for study, since the equilibrium (K_{eq}(**211**:**209**) = 0.057) of the reaction lies heavily in the direction of UDP-Gal*p* (**211**). The fluorinated analogues **225** and **226** were designed to test for (1) the possibility of a retro-Michael process initiated by oxidation of either the C(2)- or C(3)–OH as depicted in Scheme 41, and (2) the intermediacy of oxonium ions (**221**/**224**) in the catalysis as shown in Scheme 42. Since fluorine is chemically inert, one of the probes should not be a substrate for the mutase and could potentially serve as an inhibitor if a retro-Michael fragmentation is involved. In contrast, positioning a highly electronegative fluorine atom in close proximity to the anomeric carbon should severely retard the rate of oxonium ion formation and may lead to enzyme inactivation via trapping of an active site residue, if the second mechanism (Scheme 42) is operative.

Incubation of UDP-[2-F]Gal*f* (**225**) and UDP-[3-F]Gal*f* (**226**) with UDP-Gal*p* mutase in the presence of 20 mM $Na_2S_2O_4$ resulted in the formation of two new products, which were identified as UDP-[2-F]Gal*p* (**227**) and UDP-[3-F]Gal*p* (**228**, Fig. 13) [126]. The K_m values were determined to be 65 and 861 μM for UDP-[2-F]Gal*p* (**225**) and UDP-[3-F]Gal*p* (**226**), respectively. The corresponding k_{cat} values were found to be 0.033 and 5.7 s^{-1}. From these kinetic data, it is clear that the C(2)–OH contributes little to the overall mode of substrate binding. Conversely, substitution of a fluorine atom for the C(3)–OH resulted in a dramatically reduced binding affinity perhaps related to interruption of a hydrogen bonding network within the enzyme active site. The drastically reduced turnover rate for UDP-[2-F]Gal*p* (**225**) is consistent with the formation of an oxonium ion intermediate (such as **221**/**224**)

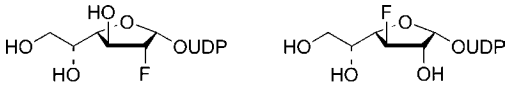

225 226

Fig. 12. Structures of UDP-[2-F]Gal*f* and UDP-[3-F]Gal*f*.

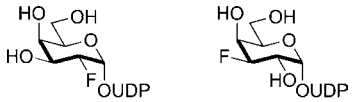

227 228

Fig. 13. Reaction products from incubation of UDP-Gal*p* mutase with UDP-[2-F]Gal*f* and UDP-[3-F]Gal*f*.

being slowed due to the electronegativity of the C(2)-F substituent. In addition, because both fluorinated substrates were recognized and processed by the enzyme, these results invalidated the proposed oxidation followed by retro-Michael pathway in Scheme 41.

However, since the overall transformation exhibits no net change in the redox state of the parties involved, how the enzyme-bound FAD plays an active role in the reaction mechanism remains elusive. It was found in a recent experiment that the mutase reconstituted with FAD or 1-deazaFAD has comparable activity, while that reconstituted with 5-deazaFAD is catalytically inactive [129]. Because 5-deazaFAD is restricted to net two-electron processes, yet FAD and 1-deazaFAD can undergo concerted two-electron as well as stepwise one-electron redox reactions, the above results support a radical mechanism for the mutase catalyzed reaction. These observations have led to a new mechanistic proposal involving one-electron transfer from the reduced FAD to **221/224** generated by C-1 elimination of UDP to give a hexose radical (**229**) and a flavin semiquinone (**230**, Scheme 43). Subsequent radical recombination leads to a coenzyme–substrate adduct (**231**) which may play a central role to facilitate the opening and recyclization of the galactose ring (**231** ↔ **232** ↔ **233**). A deprotonation step, either accompanying or following the electron transfer step, to increase the nucleophilicity of the flavin radical anion may account for the activity enhancement at pH > 8 [129]. Evidence supporting the intermediacy of **232** has recently been reported by Kiessling and co-workers [130].

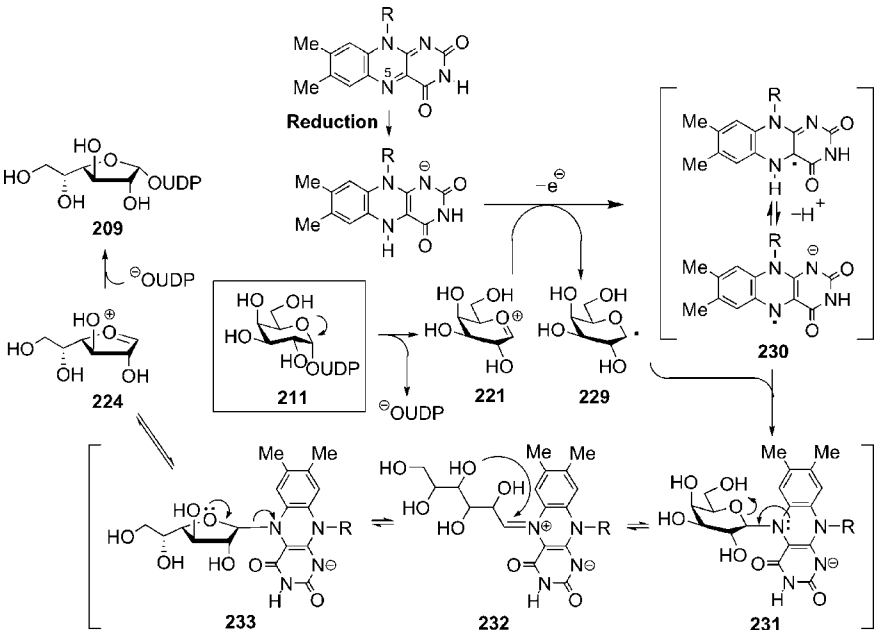

Scheme 43.

6. Conclusion

The use of fluorinated substrates has provided a wealth of information about the catalytic mechanisms of enzyme-catalyzed transformations. Assuming that the fluorinated analogue(s) is processed by the enzyme, analysis of the reaction products or inactivated enzyme complex can frequently distinguish between multiple reaction pathways. The small sampling of examples cited in this review clearly show that strategically designed fluorinated substrates can serve as mechanistic probes or inhibitors and play a key role in the elucidation of enzyme mechanisms.

Acknowledgments

The authors acknowledge the many valuable contributions made by members of the Liu group, both past and present, whose efforts are described in this review. Research in H.-w.L.'s laboratory has been supported by grants from the National Institutes of Health (GM35906, GM40541, and GM54346) and Welch Foundation (F-1511). H.-w.L. also thanks the National Institute of General Medical Sciences for a MERIT Award.

References

[1] C. Walsh, Tetrahedron 38 (1982) 871–909.
[2] C. Walsh, in: A. Meister (Ed.), Advances in Enzymology, vol. 55, John Wiley & Sons, New York, 1983, pp. 197–289.
[3] D. O'Hagan, H.S. Rzepa, J. Chem. Soc., Chem. Commun. (1997) 645–652.
[4] A. Stabel, L. Dasaradhi, D. O'Hagan, J.P. Rabe, Langmuir 11 (1995) 1427–1430.
[5] P.M. Dewick, Nat. Prod. Rep. 19 (2002) 181–222.
[6] T. Kuzuyama, H. Seto, Nat. Prod. Rep. 20 (2003) 171–183.
[7] J.W. Cornforth, R.H. Cornforth, G. Popjak, L. Yengoyan, J. Biol. Chem. 241 (1966) 3970–3987.
[8] C.D. Poulter, H.C. Rilling, Acc. Chem. Res. 11 (1978) 307–313.
[9] H.C. Rilling, K. Bloch, J. Biol. Chem. 234 (1959) 1424–1432.
[10] J.W. Cornforth, G. Popjak, Tetrahedron Lett. (1959) 29–35.
[11] C.D. Poulter, H.C. Rilling, Biochemistry 15 (1976) 1079–1083.
[12] C.D. Poulter, D.M. Satterwhite, Biochemistry 16 (1977) 5470–5478.
[13] Y. Okamoto, T. Inukai, H.C. Brown, J. Am. Chem. Soc. 80 (1958) 4969–4972.
[14] C.D. Poulter, J.C. Argyle, E.A. Mash, J. Am. Chem. Soc. 99 (1977) 957–959.
[15] C.D. Poulter, J.C. Argyle, E.A. Mash, J. Biol. Chem. 253 (1978) 7227–7233.
[16] G. Popjak, J.W. Cornforth, Biochem. J. 101 (1966) 553–568.
[17] J.E. Reardon, R.H. Abeles, J. Am. Chem. Soc. 107 (1985) 4078–4079.
[18] M. Muehlbacher, C.D. Poulter, J. Am. Chem. Soc. 107 (1985) 8307–8308.
[19] A.S. Narula, A. Rahier, P. Benveniste, P. Place, C. Anding, J. Am. Chem. Soc. 103 (1981) 2408–2409.
[20] R.M. Sandifer, M.D. Thompson, R.G. Gaughen, C.D. Poulter, J. Am. Chem. Soc. 104 (1982) 7376–7378.
[21] A. Rahier, J.C. Genot, F. Schuber, P. Benveniste, A.S. Narula, J. Biol. Chem. 259 (1984) 15215–15223.
[22] A. Rahier, M. Taton, P. Schmitt, P. Benveniste, P. Place, C. Anging, Phytochemistry 24 (1985) 1223.

[23] P. Croteau, C.J. Wheeler, R. Aksela, A.C. Oehlschlager, J. Biol. Chem. 261 (1986) 7257–7263.
[24] J.E. Reardon, R.H. Abeles, Biochemistry 25 (1986) 5609–5616.
[25] M. Muehlbacher, C.D. Poulter, Biochemistry 27 (1988) 7315–7328.
[26] C.D. Poulter, M. Muehlbacher, D.R. Davis, J. Am. Chem. Soc. 111 (1989) 3740–3742.
[27] I.P. Street, H.R. Coffman, J.A. Baker, C.D. Poulter, Biochemistry 33 (1994) 4212–4217.
[28] S.G. Withers, I.P. Street, P. Bird, D.H. Dolphin, J. Am. Chem. Soc. 109 (1987) 7530–7531.
[29] S.G. Withers, K. Rupitz, I.P. Street, J. Biol. Chem. 263 (1988) 7929–7932.
[30] S.G. Withers, I.P. Street, J. Am. Chem. Soc. 110 (1988) 8551–8553.
[31] S.G. Withers, R.A.J. Warren, I.P. Street, K. Rupitz, J.B. Kempton, R. Aebersold, J. Am. Chem. Soc. 112 (1990) 5887–5889.
[32] C. Walsh, in: Antibiotics: Actions Origins Resistance, ASM Press, Wahington DC, 2003, pp. 23–50.
[33] K.S. Anderson, J.A. Sikorski, K.A. Johnson, Biochemistry 27 (1988) 7395–7406.
[34] K.S. Anderson, J.A. Sikorski, A.J. Benesi, K.A. Johnson, J. Am. Chem. Soc. 110 (1988) 6577–6579.
[35] J.L. Marquardt, E.D. Brown, C.T. Walsh, K.S. Anderson, J. Am. Chem. Soc. 115 (1993) 10398–10399.
[36] D.H. Kim, W.J. Lees, C.T. Walsh, J. Am. Chem. Soc. 116 (1994) 6478–6479.
[37] E.D. Brown, J.L. Marquardt, J.P. Lee, C.T. Walsh, K.S. Anderson, Biochemistry 33 (1994) 10638–10645.
[38] D.H. Kim, W.J. Lees, T.M. Haley, C.T. Walsh, J. Am. Chem. Soc. 117 (1995) 1494–1502.
[39] T.P. Begley, Nat. Prod. Rep. 13 (1996) 177.
[40] J.J. Reddick, R. Nicewonger, T.P. Begley, Biochemistry 40 (2001) 10095–10102.
[41] D.W. Grogan, J.E. Cronan Jr., J. Bacteriol. 158 (1984) 286–295.
[42] D.W. Grogan, J.E. Cronan Jr., J. Bacteriol. 166 (1986) 872–877.
[43] M. Monteoliva-Sanchez, A. Ramos-Cormenzana, N.J. Russell, J. Gen. Microbiol. 139 (1993) 1877–1884.
[44] A.-Y. Wang, J.E. Cronan, Mol. Microbiol. 11 (1994) 1009–1017.
[45] M.S. Glickman, J.S. Cox, W.R. Jacobs Jr., Mol. Cell 5 (2000) 717–727.
[46] E. Lederer, Q. Rev. Chem. Soc. 23 (1969) 453–481.
[47] J.H. Law, Acc. Chem. Res. 4 (1971) 199–203.
[48] P.H. Buist, D.B. Maclean, Can. J. Chem. 59 (1981) 828–838.
[49] Y. Yuan, C.E. Barry III, Proc. Natl. Acad. Sci. USA 93 (1996) 12828–12833.
[50] T. Cohen, G. Herman, T.M. Chapman, D. Kuhn, J. Am. Chem. Soc. 96 (1974) 5627–5628.
[51] E.J. Molitor, B.M. Paschal, H.-w. Liu, ChemBioChem 4 (2003) 1352–1356.
[52] M.I.S. Lomax, G.R. Greenberg, J. Biol. Chem. 242 (1967) 109–113.
[53] M.I.S. Lomax, G.R. Greenberg, J. Biol. Chem. 242 (1967) 1302–1306.
[54] D.V. Santi, C.S. McHenry, H. Sommer, Biochemistry 13 (1974) 471–481.
[55] R.G. Kallen, W.P. Jencks, J. Biol. Chem. 241 (1966) 5851–5863.
[56] S.J. Benkovic, P.A. Benkovic, D.R. Comfort, J. Am. Chem. Soc. 91 (1969) 5270–5279.
[57] D.V. Santi, C.F. Brewer, Biochemistry 12 (1973) 2416–2424.
[58] A.L. Pogolotti, D.V. Santi, Biochemistry 13 (1974) 456–466.
[59] W. Huang, D.V. Santi, J. Biol. Chem. 269 (1994) 31327–31329.
[60] C.W. Carreras, D.V. Santi, Annu. Rev. Biochem. 34 (1995) 721–762.
[61] D.V. Santi, A.L. Pogolotti, J. Heterocyclic Chem. 8 (1971) 265–272.
[62] E.J. Pastore, M. Friedkin, J. Biol. Chem. 237 (1962) 3802–3809.
[63] M.G. Kunitani, D.V. Santi, Biochemistry 19 (1980) 1271–1275.
[64] J.E. Barrett, D.A. Maltby, D.V. Santi, P.G. Schultz, J. Am. Chem. Soc. 120 (1998) 449–450.
[65] L.L. Engel, Handbook Physiol. Sect. 7: Endocrinol. 2 (1972) 467–483.
[66] P.A. Marcotte, C.H. Robinson, Biochemistry 21 (1982) 2773–2778.
[67] W.G. Kelly, D. Judd, A. Stolee, Biochemistry 16 (1977) 140–145.
[68] H.-w. Liu, J.S. Thorson, Annu. Rev. Microbiol. 48 (1994) 223–256.
[69] X. He, J.S. Thorson, H.-w. Liu, Biochemistry 35 (1996) 4721–4731.
[70] Y. Yuan, R.N. Russell, J.S. Thorson, L.-d. Liu, H.-w. Liu, J. Biol. Chem. 267 (1992) 5868–5875.
[71] C.-w.T. Chang, X.H. Chen, H.-w. Liu, J. Am. Chem. Soc. 120 (1998) 9698–9699.

[72] H. Seto, T. Hidaka, T. Kuzuyama, S. Shibahara, T. Usui, O. Sakanaka, S. Imai, J Antibiot. 44 (1991) 1286–1288.
[73] F.J. Hammerschmidt, J. Chem. Soc., Perkin Trans. 1 (1991) 1993–1996.
[74] P. Liu, K. Murakami, T. Seki, X. He, S.-M. Yeung, T. Kuzuyama, H. Seto, H.-w. Liu, J. Am. Chem. Soc. 123 (2001) 4619–4620.
[75] A.G. Prescott, M.D. Lloyd, Nat. Prod. Rep. 17 (2000) 367–383.
[76] Z. Zhao, P. Liu, K. Murakami, T. Kuzuyama, H. Seto, H.-w. Liu, Angew. Chem. Int. Ed. 41 (2002) 4529–4532.
[77] C. Leriche, X. He, C.-w.T. Chang, H.-w. Liu, J. Am. Chem. Soc. 125 (2003) 6348–6349.
[78] T.M. Weigel, L.-d. Liu, H.-w. Liu, Biochemistry 31 (1992) 2129–2139.
[79] R.K. Hill, M.G. Bock, J. Am. Chem. Soc. 100 (1978) 637–639.
[80] E. Toromanoff, C.R. Seances, Acad. Sci. Ser. C 290 (1980) 81–84.
[81] P. Macheroux, J. Schmid, N. Amrhein, A. Schaller, Planta 207 (1999) 325–334.
[82] H.G. Floss, D.K. Onderka, M. Carroll, J. Biol. Chem. 247 (1972) 736–744.
[83] B. Ganem, Tetrahedron 34 (1978) 3353–3383.
[84] R.B. Croteau, J.J. Shaskus, B. Renstron, N.M. Felton, D.E. Cane, A. Saito, C. Chang, Biochemistry 24 (1985) 7077–7085.
[85] D.E. Cane, R. Iyengar, M.-S. Shiao, J. Am. Chem. Soc. 103 (1981) 914–931.
[86] D.E. Cane, A. Saito, R. Croteau, J. Shaskus, M. Felton, J. Am. Chem. Soc. 104 (1982) 5831–5833.
[87] D.E. Cane, Tetrahedron 36 (1980) 1109–1159.
[88] P.A. Bartlett, K.L. McLaren, D.G. Alberg, A. Fassler, R. Nyfeler, C.T. Lauhon, C.B. Grissom, Proc. Soc. Chem. Ind. Pesticides Group Meeting, BCPC Monograph 42 (1989) 155–170.
[89] W. Thiel, J. Am. Chem. Soc. 103 (1981) 1413–1420.
[90] G. Koltzenburg, G. Behrens, D. Schulte-Frohlinde, J. Am. Chem. Soc. 104 (1982) 7311–7312.
[91] A. Osborne, R.N.F. Thorneley, C. Abell, S. Bornemann, J. Biol. Chem. 275 (2000) 35825–35830.
[92] P.A. Bartlett, U. Maitra, P.M. Chouinard, J. Am. Chem. Soc. 108 (1986) 8068–8071.
[93] M.N. Ramjee, J.R. Coggins, T.R. Hawkes, D.J. Lowe, R.N.F. Thorneley, J. Am. Chem. Soc. 113 (1991) 8566–8567.
[94] M.N. Ramjee, S. Balasubramanian, C. Abell, J.R. Coggins, G.M. Davies, T.R. Hawkes, D.J. Lowe, R.N.F. Thorneley, J. Am. Chem. Soc. 114 (1992) 3151–3153.
[95] C.T. Lauhon, P.A. Bartlett, Biochemistry 33 (1994) 14100–14108.
[96] S. Bornemann, M.K. Ramjee, S. Balasubramanian, C. Abell, J.R. Coggins, D.J. Lowe, R.N.F. Thorneley, J. Biol. Chem. 270 (1995) 22811–22815.
[97] S. Bornemann, M.-E. Theoclitou, M. Brune, M.R. Webb, R.N.F. Thorneley, C. Abell, Bioorganic Chem. 28 (2000) 191–204.
[98] T.M. Weigel, V.P. Miller, H.-w. Liu, Biochemistry 31 (1992) 2140–2147.
[99] J.S. Thorson, H.-w. Liu, J. Am. Chem. Soc. 115 (1993) 7539–7540.
[100] J.S. Thorson, H.-w. Liu, J. Am. Chem. Soc. 115 (1993) 12177–12178.
[101] G.T. Gassner, D.A. Johnson, H.-w. Liu, D.P. Ballou, Biochemistry 35 (1996) 7752–7761.
[102] X. He, O. Ploux, H.-w. Liu, Biochemistry 35 (1996) 16412–16420.
[103] P.A. Pieper, D.-y. Yang, H.-q. Zhou, H.-w. Liu, J. Am. Chem. Soc. 119 (1997) 1809–1817.
[104] C.-W.T. Chang, D.A. Johnson, V. Bandarian, H. Zhou, R. LoBrutto, G.H. Reed, H.-w. Liu, J. Am. Chem. Soc. 122 (2000) 4239–4240.
[105] A.E. Evangelopoulos, in: Chemical and Biological Aspects of Vitamin B_6 Catalysis, A.R. Liss, New York, 1984.
[106] D. Dolphin, R. Poulson, O. Avramovic (Eds.), Vitamin B_6 Pyridoxal Phosphate, Chemical, Biochemical, and Medical Aspects, Wiley-Interscience, New York, 1986, Parts A and B.
[107] P.A. Frey, S.J. Booker, Adv. Protein Chem. 58 (2001) 1–45.
[108] P.A. Frey, C.H. Chang, M.D. Ballinger, G.H. Reed, Methods Enzymol. 354 (2002) 426–435.
[109] D.A. Johnson, G.T. Gassner, V. Bandarian, F.J. Ruzicka, D.P. Ballou, G.H. Reed, H.-w. Liu, Biochemistry 35 (1996) 15846–15856.
[110] D.-y. Yang, Y. Shih, H.-w. Liu, J. Org. Chem. 56 (1991) 2940–2946.

[111] A. Carrington, A.D. McLachlan, in: Introduction to Magnetic Resonance, Harper and Row, New York, 1967, pp. 79–80.
[112] J.R. Norris, R.A. Uphaus, H.L. Crespi, J. Katz, Proc. Natl. Acad. Sci. USA 68 (1971) 625–628.
[113] W.B. Mims, in: Electron Paramagnetic Resonance, Plenum Press, New York, 1972, pp. 263–351.
[114] T.M. Hallis, H.-w. Liu, J. Am. Chem. Soc. 121 (1999) 6765–6766.
[115] T.M. Hallis, Z. Zhao, H.-w. Liu, J. Am. Chem. Soc. 122 (2000) 10493–10503.
[116] P.A. FreyComplex Pyridine Nucleotide-Dependent Transformations, vol. 1, John Wiley & Sons, New York, 1987, pp. 462–510.
[117] A.J. Bauer, I. Rayment, P.A. Frey, H.M. Holden, Proteins 12 (1992) 372–381.
[118] J.R. Burke, P.A. Frey, Biochemistry 32 (1993) 13220–13230.
[119] J.B. Thoden, P.A. Frey, H.M. Holden, Biochemistry 35 (1996) 5137–5144.
[120] P.A. Frey, FASEB 10 (1996) 461–470.
[121] H. Chen, Z. Guo, H.-w. Liu, J. Am. Chem. Soc. 120 (1998) 11796–11797.
[122] Z. Zhao, H.-w. Liu, J. Org. Chem. 66 (2001) 6810–6815.
[123] R.M. de Lederkremer, W. Colli, Glycobiology 5 (1995) 547–552.
[124] P.J. Brennan, H. Nikaido, Annu. Rev. Biochem. 64 (1995) 29–63.
[125] C. Whitfield, Trends Microbiol. 3 (1995) 178–185.
[126] Q. Zhang, H.-w. Liu, J. Am. Chem. Soc. 123 (2001) 6756–6766.
[127] J.N. Barlow, M.E. Girvin, J.S. Blanchard, J. Am. Chem. Soc. 121 (1999) 6968–6969.
[128] Q. Zhang, H.-w. Liu, J. Am. Chem. Soc. 122 (2000) 9065–9070.
[129] Z. Huang, Q. Zhang, H.-w. Liu, Bioorganic Chem. 31 (2003) 494–502.
[130] M. Soltero-Higgin, E.E. Carlson, T.D. Gruber, L.L. Kiessling, Nat. Struct. Mol. Biol. 11 (2004) 539–543.